

THE ANTENNA LABORATORY

RESEARCH ACTIVITIES in ---

Automatic Controls *Antennas* *Echo Area Studies*
Microwave Circuits *Astronautics* *E M Field Theory*
Terrain Investigations *Radomes* *Systems Analysis*
Wave Propagation *Submillimeter Applications*

FACILITY FORM 602

N66-16699

(ACCESSION NUMBER)

(THRU)

55

(PAGES)

1

(CODE)

CR 70047

(NASA CR OR TMX OR AD NUMBER)

07

(CATEGORY)

COUPLING BETWEEN PARALLEL-PLATE WAVEGUIDES BY WEDGE DIFFRACTION TECHNIQUES

L. L. Tsai; R. C. Rudduck;
R. B. Dybdal

GPO PRICE \$ _____

CFSTI PRICE(S) \$ _____

Grant Number NsG-448

Hard copy (HC) \$ 3.00

Microfiche (MF) .57

ff 653 July 65

1691-17

20 October 1965

Prepared for:
 National Aeronautics and Space Administration
 Office of Grants and Research Contracts
 Washington, D. C.

Department of ELECTRICAL ENGINEERING



THE OHIO STATE UNIVERSITY
 RESEARCH FOUNDATION
 Columbus, Ohio

NOTICES

When Government drawings, specifications, or other data are used for any purpose other than in connection with a definitely related Government procurement operation, the United States Government thereby incurs no responsibility nor any obligation whatsoever, and the fact that the Government may have formulated, furnished, or in any way supplied the said drawings, specifications, or other data, is not to be regarded by implication or otherwise as in any manner licensing the holder or any other person or corporation, or conveying any rights or permission to manufacture, use, or sell any patented invention that may in any way be related thereto.

The Government has the right to reproduce, use, and distribute this report for governmental purposes in accordance with the contract under which the report was produced. To protect the proprietary interests of the contractor and to avoid jeopardy of its obligations to the Government, the report may not be released for non-governmental use such as might constitute general publication without the express prior consent of The Ohio State University Research Foundation.

Qualified requesters may obtain copies of this report from the Defense Documentation Center, Cameron Station, Alexandria, Virginia. Department of Defense contractors must be established for DDC services, or have their "need-to-know" certified by the cognizant military agency of their project or contract.

REPORT
by
THE OHIO STATE UNIVERSITY RESEARCH FOUNDATION
COLUMBUS, OHIO 43212

Sponsor	National Aeronautics and Space Administration Office of Grants and Research Contracts Washington, D. C.
Grant Number	NsG-448
Investigation of	Spacecraft Antenna Problems
Subject of Report	Coupling Between Parallel-Plate Waveguides by Wedge Diffraction Techniques
Submitted by	L. L. Tsai; R. C. Rudduck, and R. B. Dybdal Antenna Laboratory Department of Electrical Engineering
Date	20 October 1965

ABSTRACT

N66-16699

The coupling between two parallel-plate waveguides is calculated using edge-diffraction techniques. The parallel-plate guides have arbitrary truncation angles and are formed by wedges of arbitrary angular extent. Coupling is calculated for both TEM and TE₀₁ waveguide modes with the results experimentally verified.

Author

TABLE OF CONTENTS

	Page
I. INTRODUCTION	1
II. WEDGE DIFFRACTION	1
III. MUTUAL COUPLING	6
A. <u>TEM Coupling</u>	6
B. <u>TE₀₁ Coupling</u>	15
IV. GROUND PLANE CASE	22
V. RESULTS	26
VI. CONCLUSIONS	27
APPENDIX A	42
APPENDIX B	44
REFERENCES	46

COUPLING BETWEEN PARALLEL-PLATE WAVEGUIDES BY WEDGE DIFFRACTION TECHNIQUES

I. INTRODUCTION

The coupling between two parallel-plate waveguides is analyzed by application of wedge diffraction. This technique has been successfully used to analyse the radiation patterns of parallel-plate waveguides[1,2] .

The analysis of mutual coupling problems by conventional electromagnetic theory techniques is, at best, difficult. The use of geometrical techniques for treating diffraction provides relatively simple computation of coupling[3] . The structural aspects of guide geometry and orientation, and ground plane structures are accurately included in the analysis.

II. WEDGE DIFFRACTION

The coupling between parallel-plate waveguides may be analyzed in terms of diffraction by a perfectly conducting wedge. The problem of straight edge diffraction by a wedge was first solved by Sommerfeld[4] . Pauli[5] obtained a practical formulation for the finite-angle wedge. The diffraction function V_B , introduced by Pauli, is employed in the analysis and is described in Appendix A.

The diffraction of a plane wave by a wedge is illustrated in Fig. 1. The solution to the problem may be expressed in terms of a scalar function which represents the component of the electromagnetic field normal to the plane of study. The diffracted field is given by

$$(1) \quad U_d = V_B(r, \psi - \psi_0) \mp V_B(r, \psi + \psi_0) ,$$

where the minus sign applies for the electric field polarization parallel to the edge and the plus sign applies for perpendicular polarization.

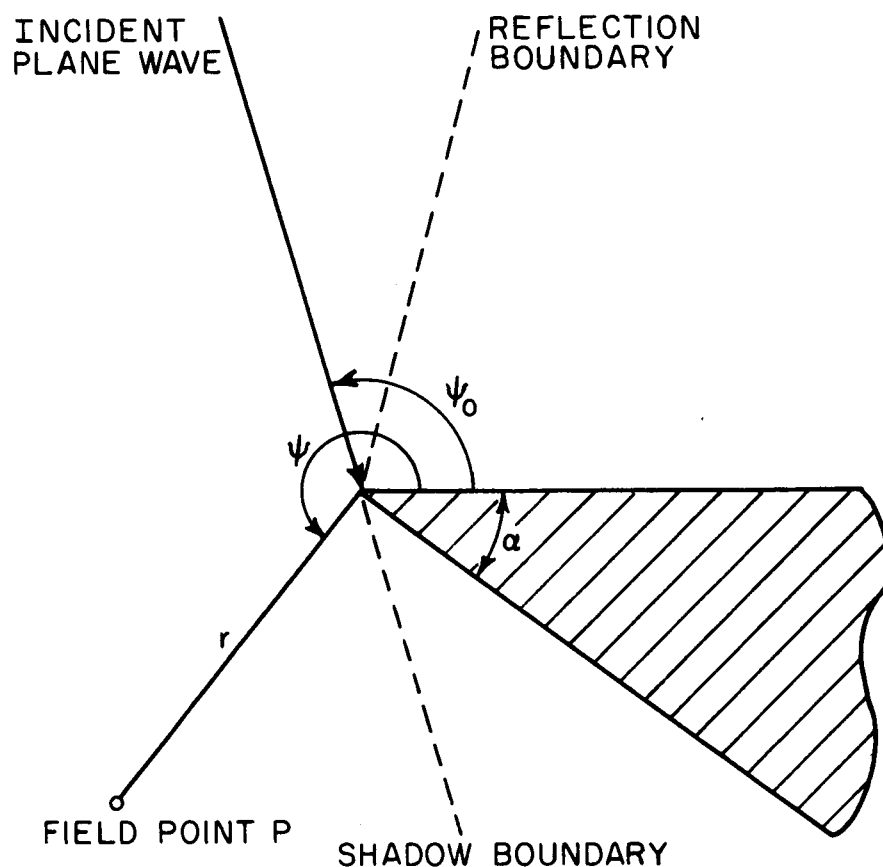


Fig. 1. Geometry for wedge diffraction.

The total field is given by

$$(2) \quad U = U_0 + U_d ,$$

where U_0 is the geometrical optics field. The three regions of the geometrical optics field are illustrated in Fig. 2. For the case of plane wave incidence, the geometrical optics fields are given by

$$(3a) \quad U_0 = e^{-jkr \cos(\psi - \psi_0)} , \text{ incident region;}$$

$$(3b) \quad U_0 = e^{-jkr \cos(\psi - \psi_0)} + e^{-jkr \cos(\psi + \psi_0)} , \text{ incident and reflected region; and}$$

$$(3c) \quad U_0 = 0, \text{ shadow region.}$$

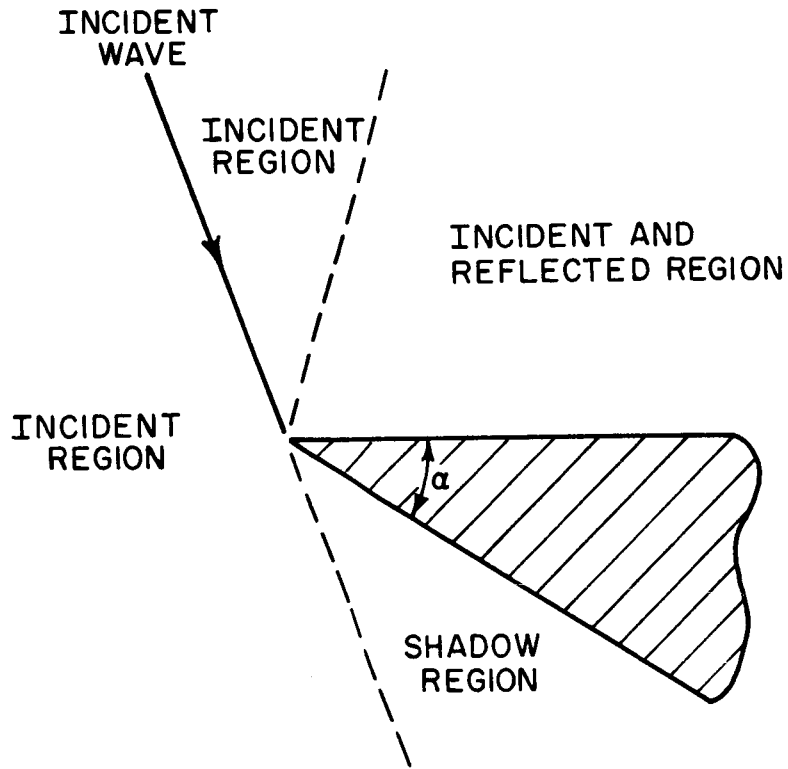


Fig. 2. Geometrical optics region.

The same convention is used for the choice of sign in Eq. (3b) as was used in Eq. (1).

The nature of the diffracted wave U_d is that of a cylindrical wave radiating from the edge. This may be seen from examination of Eq. (45) in Appendix A; at large distances from the edge the diffracted wave has the radial dependence of a cylindrical wave $e^{-jk r}/\sqrt{r}$. Consequently, a subsequent diffraction by a diffracted wave may be treated as the diffraction of a cylindrical wave by a wedge (as illustrated in Fig. 3). Two near-field formulations have been used, both of which give nearly the same results. The geometrical optics fields in each case are given by

$$(4a) \quad U_0 = \frac{e^{-jkR}}{\sqrt{R}} = \frac{e^{-jk(r^2 + r_0^2 - 2r r_0 \cos(\psi - \psi_0))^{1/2}}}{(r^2 + r_0^2 - 2r r_0 \cos(\psi - \psi_0))^{1/4}},$$

incident region;

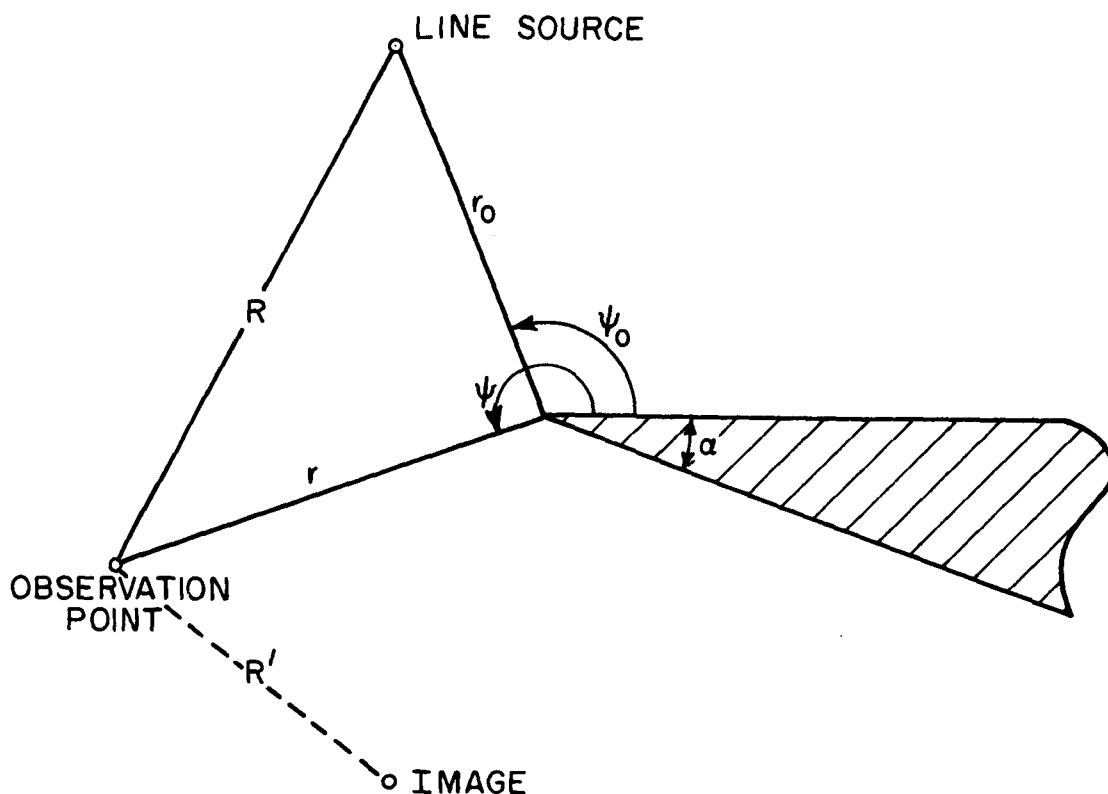


Fig. 3. Geometry of wedge and line source near field diffraction.

$$(4b) \quad U_O = \frac{e^{-jkR}}{\sqrt{R}} \pm \frac{e^{-jkR'}}{\sqrt{R'}} = \frac{e^{-jk(r^2 + r_0^2 - 2r r_0 \cos(\psi - \psi_0))^{\frac{1}{2}}}}{(r^2 + r_0^2 - 2r r_0 \cos(\psi - \psi_0))^{\frac{1}{4}}} \pm \frac{e^{-jk(r^2 + r_0^2 - 2r r_0 \cos(\psi + \psi_0))^{\frac{1}{2}}}}{(r^2 + r_0^2 - 2r r_0 \cos(\psi + \psi_0))^{\frac{1}{4}}},$$

incident and reflected region; and

$$(4c) \quad U_O = 0, \quad \text{shadow region.}$$

R and R' are the distances of the line source and its image to the observation point, respectively. The regions for the geometrical optics are the same as shown in Fig. 2.

One diffracted field formulation is obtained by modifying the solution given in Ohba[6] for the diffraction of a half-plane illuminated by a dipole source. This solution has been reduced to the two-dimensional form and extended to wedge diffraction. The diffracted wave of this formulation is thus given by

$$(5a) \quad U_d(r, r_o, \psi, \psi_o) = \frac{e^{-jk(r+r_o)}}{\sqrt{r+r_o}} e^{jk \frac{r r_o}{r+r_o}} \left[V_B\left(\frac{r r_o}{r+r_o}, \psi - \psi_o\right) \right. \\ \left. + V_B\left(\frac{r r_o}{r+r_o}, \psi + \psi_o\right) \right]$$

The plus sign applies for electric field polarization perpendicular to the edge of the wedge whereas the minus sign applies for parallel polarization. The total field is still given by Eq. (2).

The other diffracted field formulation is obtained from Born and Wolf[7] for the diffraction of a cylindrical wave by a half-plane. This formulation is extended to wedge diffraction to give the diffracted wave as

$$(5b) \quad U_d(r, r_o, \psi, \psi_o) = \frac{e^{-jk \left[R + \frac{2r r_o}{R_1 + R} \cos(\psi - \psi_o) \right]}}{\sqrt{\frac{R_1 + R}{2}}} V_B\left(\frac{2r r_o}{R_1 + R}, \psi - \psi_o\right) \\ + \frac{e^{-jk \left[R' + \frac{2r r_o}{R_1 + R'} \cos(\psi + \psi_o) \right]}}{\sqrt{\frac{R_1 + R'}{2}}} V_B\left(\frac{2r r_o}{R_1 + R'}, \psi + \psi_o\right)$$

where $R_1 = r + r_o$.

Both formulations have been extended for non-zero wedge angles to agree with Pauli's[5] formulation for plane wave diffraction ($r_o \rightarrow \infty$). However, it should be noted that both formulations are approximate. Each formulation was compared with the exact solution for diffraction of a cylindrical wave by a wedge[11] which may be evaluated for small values of r and r_o . For example, both Eqs. (5a and b) were found to be accurate within 1/2% in magnitude for $r_o = 2\lambda$ and $r < r_o$. For $r_o = 0.8\lambda$ ($r < r_o$) each formulation is usually accurate within 2 or 3%. Details of this comparison will be published in a future report.

III. MUTUAL COUPLING

The mutual coupling between the two parallel-plate waveguides shown in Fig. 4 will be analyzed by geometrical diffraction techniques. The coupling between the guides may be expressed in terms of the modal current excited in one guide by an incident wave in the other guide; the value of the incident wave may be represented by its modal current. The use of modal currents allows the phase of the coupled fields to be included in the analysis in addition to determining the coupled power. The inclusion of phase information permits multiple guide problems to be analyzed by superposition.

In order to avoid unnecessary complications of the analysis, some restriction will be placed on the geometry of Fig. 4. Namely, the orientation between the guides and the truncation angles of the guides are restricted so that edge N_1 will not be directly illuminated by guide #2, and edge N_2 will not be directly illuminated by guide #1.

Coupling in both TEM and TE_{01} waveguide modes will be considered. The TEM mode may be represented as a plane wave propagating in the guide, as shown in Fig. 5(a). For this mode the field distribution across the guide is uniform with the electric field polarization perpendicular to the guide walls. The TE_{01} mode may be represented by two plane waves bouncing in the guide, as shown in Fig. 5(b). The angle A_0 , identified in the figure, is given by

$$(6) \quad A_0 = \sin^{-1} \frac{\lambda}{2a} .$$

The field distribution across the guide is sinusoidal for the TE_{01} mode and the polarization of the electric field is parallel to the guide walls.

A. TEM Coupling

Since TEM mode coupling is easier to analyze it will be treated first. The incident power and associated modal current will first be determined for the TEM guide with a unit amplitude magnetic field directed parallel to the guide walls. The Poynting vector is uniform across the guide. Thus integration of the Poynting vector across the width of the guide yields the power flow per unit depth of guide as $Z_0 a$, where Z_0 is the impedance of free space and a is the width of the guide.

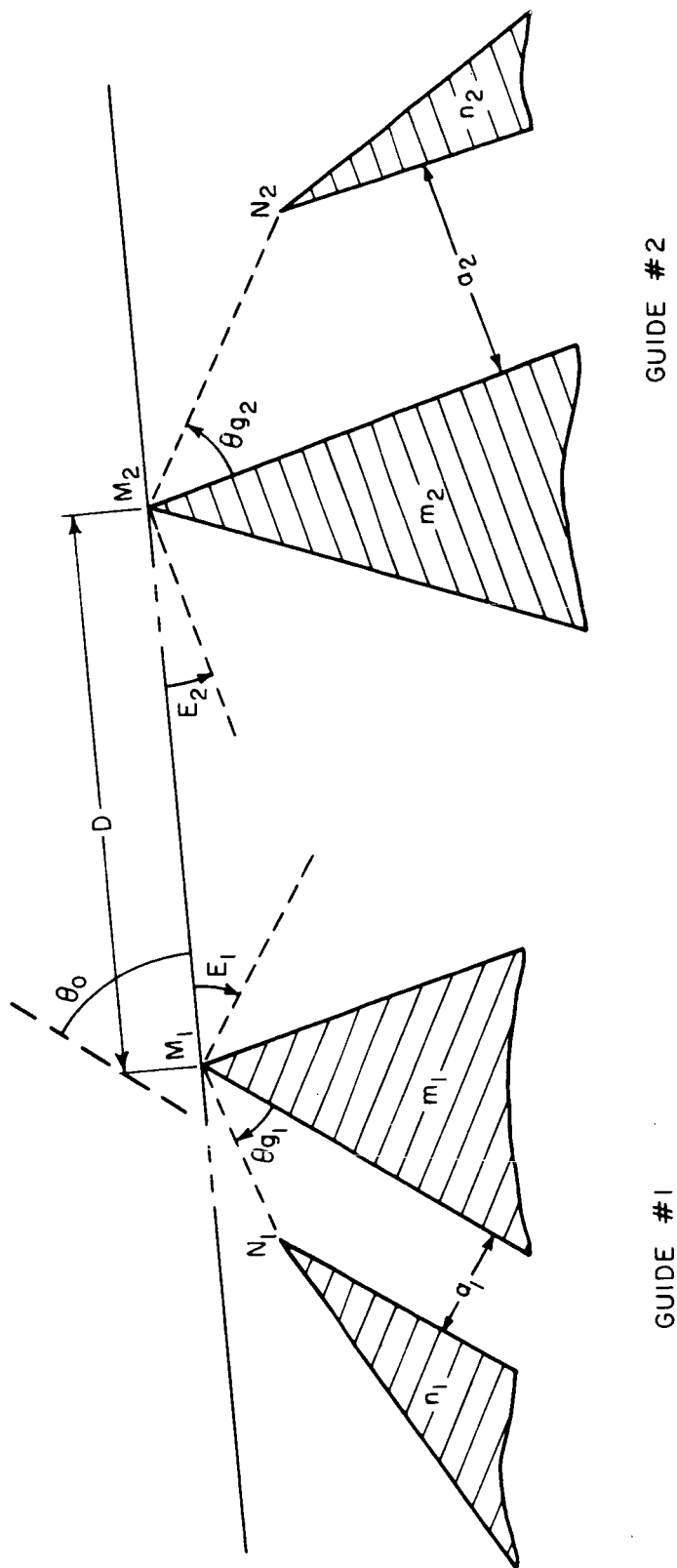


Fig. 4. Geometry for mutual coupling between parallel plate guides.

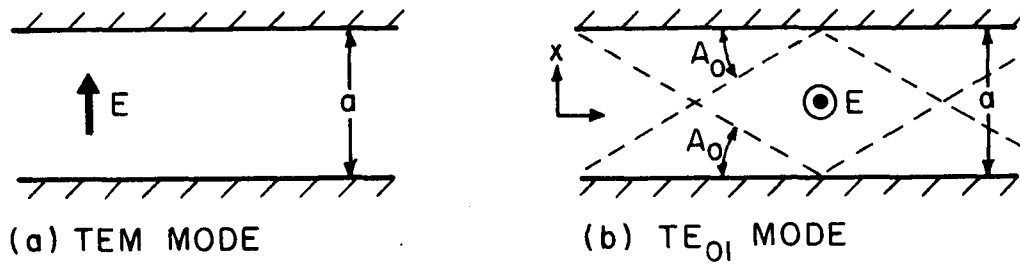


Fig. 5. TEM and TE_{01} mode propagation.

In conventional transmission line theory, power flow may be represented by the product of modal currents and voltages in the same manner as in circuit theory. Similarly, the modal quantities are related by the transmission line impedance. The transmission line impedance for the TEM mode is simply the ratio of the electric to magnetic fields, or the impedance of free space Z_0 . The field for the TEM mode will be expressed by the magnetic field because it is representable by a scalar function. Therefore, for a TEM mode guide with a guide width a , in which the magnetic field has unit amplitude and zero phase reference, the modal circuit quantities are given by

$$(7) \quad I_0 = \sqrt{a} \quad \text{and} \\ V_0 = \sqrt{a} Z_0 .$$

Since the impedance of a TEM guide is Z_0 , the mutual coupling between TEM guides can then be represented simply as a ratio of modal currents. The square of this ratio will give the power coupled.

The mutual coupling problem will be solved in essentially three steps. First, guide 1, the transmitting guide, will be replaced by an equivalent line source. Next, the response of guide 2, the receiving guide, to a line source will be determined by application of reciprocity. Then by combining these two steps, mutual coupling, or the response of guide 2 to guide 1, will be obtained. Mutual coupling can thus be expressed as

$$\begin{aligned} & \frac{\text{modal current in guide 2}}{\text{equivalent line source current of guide 1}} \\ & \times \frac{\text{equivalent line source current in guide 1}}{\text{modal current in guide 1}} \end{aligned}$$

STEP 1: Substitution of Guide 1, the transmitting guide, by an equivalent line source.

The field radiated by guide 1 (in Fig. 4) in the direction θ_0 of guide 2 is accurately given by the singly and doubly diffracted rays from edge M_1 . For an incident wave with a unit magnetic field the singly diffracted ray may be obtained from Eq. (44) as

$$(8) \quad V_B(r, \frac{3}{2}\pi - E_1, m_1) = \frac{e^{-j\left(kr + \frac{\pi}{4}\right)}}{\sqrt{2\pi kr}} \cdot \frac{\frac{1}{m_1} \sin \frac{\pi}{m_1}}{\cos \frac{\pi}{m_1} - \cos \frac{\frac{3}{2}\pi - E_1}{m_1}},$$

where the asymptotic form of V_B given in Eq. (45) is employed.

The doubly diffracted wave from edge M_1 is caused by the singly diffracted ray from edge N_1 in the direction of edge M_1 . This singly diffracted ray is given by

$$(9) \quad V_B(r, \pi - \theta_{g1}, n_1) \times e^{jka_1 \cot \theta_{g1}} \\ = \frac{e^{-j\left(kr + \frac{\pi}{4}\right)}}{\sqrt{2\pi kr}} \cdot \frac{\frac{1}{n_1} \sin \frac{\pi}{n_1}}{\cos \frac{\pi}{n_1} - \cos \frac{\pi - \theta_{g1}}{n_1}} e^{jka_1 \cot \theta_{g1}},$$

where the exponential term $e^{jka_1 \cot \theta_{g1}}$ is the result of referring the incident wave to edge M_1 . The resulting doubly diffracted ray in the direction of the second guide is obtained by Eq. (5a) as

$$(10) \quad \frac{e^{-j\frac{\pi}{4}}}{2\pi} e^{jk \frac{ra_1}{r+a_1}} \frac{e^{-jk(r+a_1)}}{\sqrt{\frac{r+a_1}{\lambda}}} \left(\frac{\frac{1}{n_1} \sin \frac{\pi}{n_1}}{\cos \frac{\pi}{n_1} - \cos \frac{\pi - \theta_{g1}}{n_1}} \right) e^{jka_1 \cot \theta_{g1}}$$

$$(10) \quad \times \left[V_B \left(\frac{a_1}{\sin \theta_{g1}}, \frac{3}{2} \pi - E_1 - \theta_{g1}, m_1 \right) + V_B \left(\frac{a_1}{\sin \theta_{g1}}, \frac{3}{2} \pi - E_1 + \theta_{g1}, m_1 \right) \right] \quad \text{cont.}$$

The singly and doubly diffracted rays are as shown in Fig. 6.

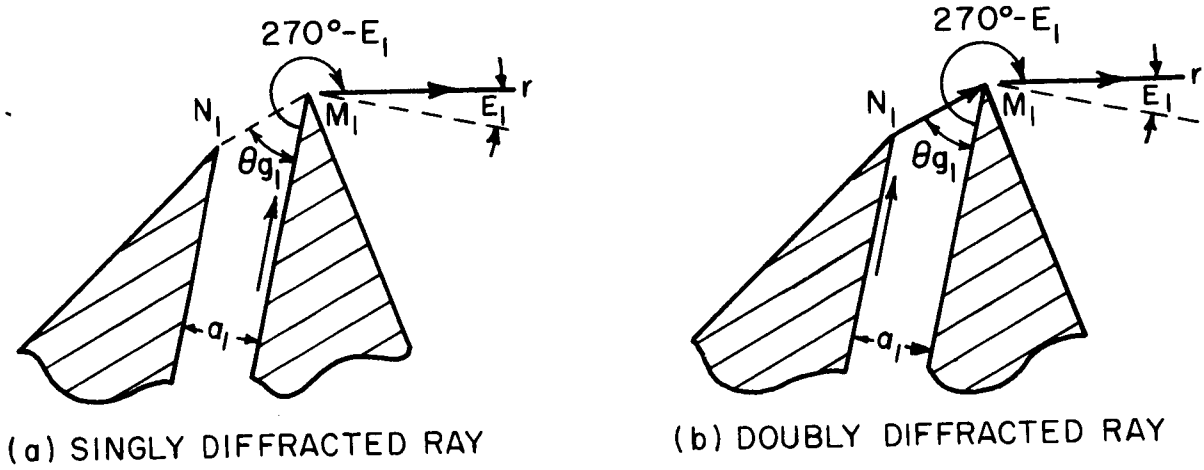


Fig. 6. Singly and doubly diffracted rays for the TEM mode.

Ignoring higher-order diffractions, the magnetic field intensity radiated in the direction of guide 2 by guide 1 with modal current $\sqrt{a_1}$ may be expressed in far-field form as

$$(11) \quad H_{T1}(\theta_0) = \frac{\sqrt{\lambda}}{2\pi} e^{-j\frac{\pi}{4}} \frac{e^{-jkr}}{\sqrt{r}} \left\{ \frac{\frac{1}{m_1} \sin \frac{\pi}{m_1}}{\cos \frac{\pi}{m_1} - \cos \frac{3/2 \pi - E_1}{m_1}} + \left(\frac{\frac{1}{n_1} \sin \frac{\pi}{n_1}}{\cos \frac{\pi}{n_1} - \cos \frac{\pi - \theta_{g1}}{n_1}} \right) e^{jka_1 \cot \theta_{g1}} \right. \\ \left. \left[V_B \left(\frac{a_1}{\sin \theta_{g1}}, \frac{3}{2} \pi - E_1 - \theta_{g1}, m_1 \right) + V_B \left(\frac{a_1}{\sin \theta_{g1}}, \frac{3}{2} \pi - E_1 + \theta_{g1}, m_1 \right) \right] \right\}.$$

An equivalent line source with an omnidirectional radiation pattern but with its radiated field exactly equal in amplitude and phase to the field of guide 1 in the direction of guide 2 (i. e., θ_0) may now be introduced to replace guide 1. Therefore in this analysis guide 1 is replaced by a single line source located at edge M_1 that radiates a field given by

$$(12) \quad I_{eq} \frac{e^{-jkr + j\frac{\pi}{4}}}{\sqrt{2\pi r}} = H_{T1}(\theta_0) = D_{T1}(\theta_0) \frac{e^{-jkr}}{\sqrt{r}},$$

where I_{eq} is the modal current of the equivalent line source. The characteristic impedance of the line source is chosen to be the same as that of the TEM guide, Z_0 . The $e^{-j(kr - \pi/4)}$ phase factor in Eq. (12) results from the fact that the field radiated by the line source modal current must be consistent with the field radiated by a TEM waveguide modal current. This phase factor is derived in Appendix B.

The modal current of the equivalent line source is thus obtained from Eq. (12) as

$$(13) \quad I_{eq} = \sqrt{2\pi} D_{T1}(\theta_0) e^{-j\frac{\pi}{4}}.$$

As shown in Fig. 7, the transmitting guide (guide 1) has been replaced by an equivalent line source with modal current I_{eq} such that the same response is obtained in guide 2.

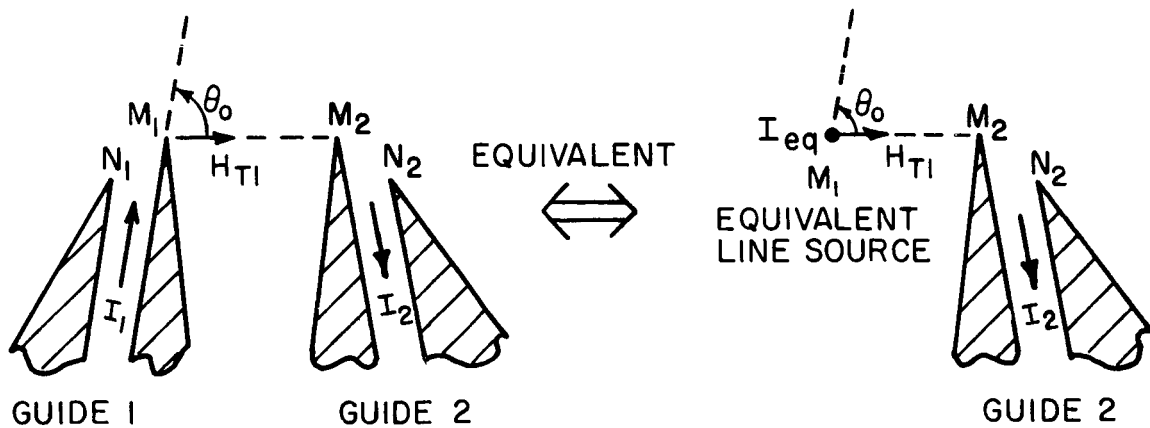


Fig. 7. Substituting guide 1 by an equivalent line source.

STEP: 2 Response of Guide 2 to a line source.

By reciprocity, the response of a guide to a line source is equal to the response of that line source to the guide; this is shown diagrammatically in Fig. 8. In Fig. 8(a), a line source with modal current I_T located at point Q transmits a power P_T . Guide 2 receives a power P_R with associated modal current I_R from the line source. In the reciprocal situation shown in Fig. 8(b), guide 2 transmits power P_T with associated modal current I_T . The line source receives power P_R with associated modal current I_R . The power received by the line source in Fig. 8(b) is given by

$$(14) \quad P_R = \frac{\lambda}{2\pi} |H_T(Q)|^2 Z_0 ,$$

where $\lambda/2\pi$ is the effective aperture of a line source and $H_T(Q)$ is the field at point Q due to the guide. Thus the modal current received by the line source is given by

$$(15) \quad I_R = \sqrt{\frac{\lambda}{2\pi}} H_T(Q) ,$$

where the characteristic impedance of the line source is Z_0 .

The field $H_T(Q)$ at point Q due to guide 2 may be computed by use of Eqs. (1) and (5). For an incident wave with a unit magnetic field in the

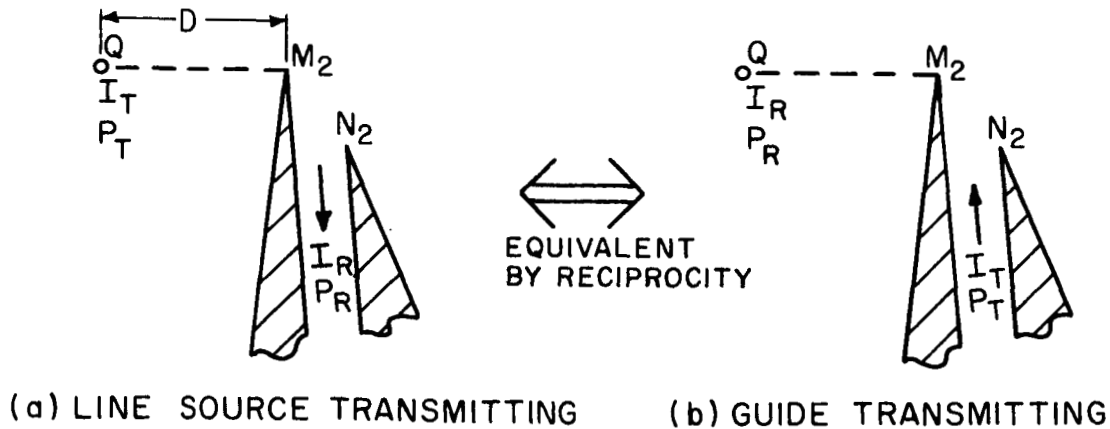


Fig. 8. Application of reciprocity to find response of a guide to a line source.

guide the singly diffracted field at point Q from edge M_2 is obtained as

$$(16) \quad SD = V_B(D, \frac{3}{2} \pi - E_2, m_2) \quad .$$

The doubly diffracted field from edge M_2 results from the singly diffracted ray from edge N_2 and is given by

$$(17) \quad DD = e^{jk a_2 \cot \theta_{g2}} \left(\frac{\sqrt{\lambda}}{2\pi} \right) \left(\frac{\frac{1}{n_2} \sin \frac{\pi}{n_2} e^{-j \frac{\pi}{4}}}{\cos \frac{\pi}{n_2} - \cos \frac{\pi - \theta_{g2}}{n_2}} \right) \cdot U_d \left(D, \frac{a_2}{\sin \theta_{g2}}, \frac{3}{2} \pi - E_2, \theta_{g2} \right) \quad .$$

Thus the total field at point Q caused by guide 2 is given by

$$(18) \quad H_{T_2}(Q) = V_B(D, \frac{3}{2} \pi - E_2, m_2) + \left(\frac{e^{jk \left(\frac{a_2}{a_2 - D \sin \theta_{g2}} - \left(\frac{a_2}{\sin \theta_{g2}} + D \right) \right)}}{2\pi \sqrt{\frac{a_2 + D \sin \theta_{g2}}{\lambda \sin \theta_{g2}}}} \right) e^{jk a_2 \cot \theta_{g2}} \times \left(\frac{\frac{1}{n_2} \sin \frac{\pi}{n_2} e^{-j \frac{\pi}{4}}}{\cos \frac{\pi}{n_2} - \cos \frac{\pi - \theta_{g2}}{n_2}} \right) \times \left[V_B \left(\frac{a_2 D}{a_2 + D \sin \theta_{g2}}, \frac{3}{2} \pi - E_2 - \theta_{g2}, m_2 \right) + V_B \left(\frac{a_2 D}{a_2 + D \sin \theta_{g2}}, \frac{3}{2} \pi - E_2 + \theta_{g2}, m_2 \right) \right] \quad ,$$

where the modal current of the source is $\sqrt{a_2}$. Therefore, the response of the line source at point Q to guide 2 is given by the modal current ratio

$$(19) \quad \frac{I_R}{I_T} = \sqrt{\frac{\lambda}{2\pi a_2}} H_{T_2}(Q) .$$

By reciprocity, Eq. (19) gives the response I_R of guide 2 to a line source with a transmitting modal current I_T .

The near-field formulation of Eq. (5a) is used in the above equations for the doubly diffracted terms. Computations were made using both near-field formulations. The difference in the doubly diffracted terms as computed by the two diffraction forms was found to be negligible. In fact, this effect is second-order relative to the order of approximating the diffraction of the guide as that of line source diffraction.

STEP 3: Mutual Coupling

The last step remains in combining the results of the previous two to obtain mutual coupling, defined as the ratio between modal currents in the transmitting and receiving guides, namely, I_2/I_1 . The modal current response I_2 of guide 2 is given by I_R of Eq. (19) with the modal current I_T specified by the modal current I_{eq} of the equivalent line source. Thus, combining Eqs. (13) and (19) the mutual coupling between the parallel-plate TEM guides of Fig. 4 is given by

$$(20) \quad \frac{I_2 \text{ (modal current received in guide 2)}}{I_1 \text{ (modal current transmitted by guide 1)}} = \sqrt{\frac{\lambda}{a_1 a_2}} D_{T_1}(\theta_0) H_{T_2}(Q) e^{-j\frac{\pi}{4}}$$

$$= \frac{\lambda e^{-j\frac{\pi}{2}}}{2\pi\sqrt{a_1 a_2}} \left\{ \frac{\frac{1}{m_1} \sin \frac{\pi}{m_1}}{\cos \frac{\pi}{m_1} - \cos \frac{3/2\pi - E_1}{m_1}} \right.$$

$$\left. + \left(\frac{\frac{1}{n_1} \sin \frac{\pi}{n_1}}{\cos \frac{\pi}{n_1} - \cos \frac{\pi - \theta_{g1}}{n_1}} \right) \right. \quad \text{(equation continued on next page)}$$

(20)
cont.

$$\begin{aligned}
& \cdot e^{jka_1 \cot \theta_{g1}} \left[V_B \left(\frac{a_1}{\sin \theta_{g1}}, \frac{3}{2} \pi - E_1 - \theta_{g1}, m_1 \right) \right. \\
& \left. + V_B \left(\frac{a_1}{\sin \theta_{g1}}, \frac{3}{2} \pi - E_1 + \theta_{g1}, m_1 \right) \right] \cdot \left\{ V_B(D, \frac{3}{2} \pi - E_2, m_2) \right. \\
& \left. + \frac{e^{jk \left(\frac{a_2 D}{a_2 + D \sin \theta_{g2}} - \left(\frac{a_2}{\sin \theta_{g2}} + D \right) \right)}}{2\pi \sqrt{\frac{a_2 + D \sin \theta_{g2}}{\lambda \sin \theta_{g2}}}} \right\} \\
& \cdot e^{jka_2 \cot \theta_{g2}} \left(\frac{\frac{1}{n_2} \sin \frac{\pi}{n_2}}{\cos \frac{\pi}{n_2} - \cos \frac{\pi - \theta_{g2}}{n_2}} \right) e^{-j \frac{\pi}{4}} \\
& \cdot \left[V_B \left(\frac{a_2 D}{a_2 + D \sin \theta_{g2}}, \frac{3}{2} \pi - E_2 - \theta_{g2}, m_2 \right) \right. \\
& \left. + V_B \left(\frac{a_2 D}{a_2 + D \sin \theta_{g2}}, \frac{3}{2} \pi - E_2 + \theta_{g2}, m_2 \right) \right] \cdot
\end{aligned}$$

$D_{T_1}(\theta_0)$ is the diffraction coefficient of the transmitting guide as given by Eqs. (11) and (12). $H_{T_2}(Q)$ is the field of the receiving guide at point Q as given in Eq. (18). The power coupled between the two guides is given by

$$(21) \quad \frac{P_2}{P_1} = \left| \frac{I_2}{I_1} \right|^2.$$

B. TE₀₁ Coupling

The analysis of mutual coupling for the TE₀₁ mode is basically the same as that for the TEM mode. The field will be expressed in terms of

the electric field because it may be represented by a scalar function for the TE_{01} mode. As shown in Fig. 5(b), the electric field across the guide varies as $\cos 2\pi x/a$. For a unit amplitude electric field in each plane-wave component, integration of the Poynting vector across the guide width yields a power flow of $2 Y_0 a \cos A_0$. Thus the associated modal voltage is

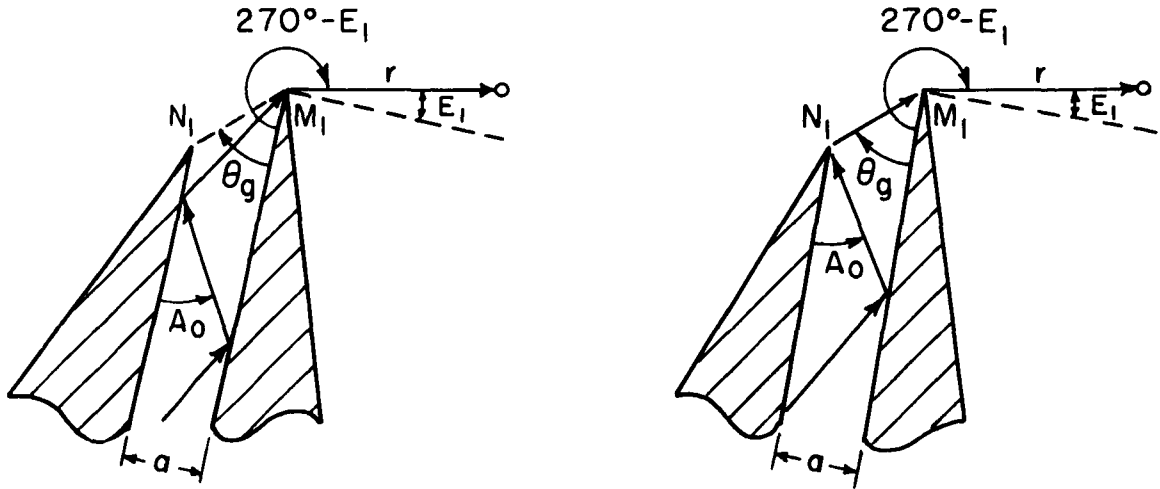
$$(22) \quad V_0 = \sqrt{2a \frac{Y_0}{Y_g} \cos A_0} ,$$

where Y_0 is the free-space admittance and Y_g is the guide admittance for the TE_{01} mode.

The mutual coupling problem to be solved has the same general geometry as given in Fig. 4. An additional restriction is that $\theta_{g1} > A_{01}$ and $\theta_{g2} > A_{02}$ so that edges M_1 and M_2 will be illuminated by the incident fields. The same three steps used in the TEM analysis are used to obtain the solution.

STEP 1: Substitution of Guide 1 by an equivalent line source

The singly and doubly diffracted rays for the TE_{01} mode are shown in Fig. 9. The singly diffracted field from edge M_1 is given by



(a) SINGLY DIFFRACTED RAY

(b) DOUBLY DIFFRACTED RAY

Fig. 9. Singly and doubly diffracted ray for the TE_{01} mode.

$$\begin{aligned}
(23) \quad & V_B(r, \frac{3}{2}\pi - E_1 - A_{01}, m_1) - V_B(r, \frac{3}{2}\pi - E_1 + A_{01}, m_1) \\
& = \left(\frac{\frac{1}{m_1} \sin \frac{\pi}{m_1}}{\cos \frac{\pi}{m_1} - \cos \frac{3/2\pi - E_1 - A_{01}}{m_1}} - \frac{\frac{1}{m_1} \sin \frac{\pi}{m_1}}{\cos \frac{\pi}{m_1} - \cos \frac{3/2\pi - E_1 + A_{01}}{m_1}} \right) \\
& \quad \frac{e^{-j(kr + \frac{\pi}{4})}}{\sqrt{2\pi kr}},
\end{aligned}$$

where the asymptotic form of V_B given in Eq. (45) is employed. The singly diffracted wave from edge N_1 in the direction of edge M_1 is given by

$$\begin{aligned}
(24) \quad & [V_B(r, \pi - \theta_{g1} - A_{01}, n_1) - V_B(r, \pi - \theta_{g1} + A_{01}, n_1)] e^{jka_1 \cot \theta_{g1} \cos A_{01}} \\
& = \left[\frac{\frac{1}{n_1} \sin \frac{\pi}{n_1}}{\cos \frac{\pi}{n_1} - \cos \frac{\pi - \theta_{g1} - A_{01}}{n_1}} - \frac{\frac{1}{n_1} \sin \frac{\pi}{n_1}}{\cos \frac{\pi}{n_1} - \cos \frac{\pi - \theta_{g1} + A_{01}}{n_1}} \right] \\
& \quad \times e^{jka_1 \cot \theta_{g1} \cos A_{01}} \times \frac{e^{-j(kr + \frac{\pi}{4})}}{\sqrt{2\pi kr}},
\end{aligned}$$

where the exponential factor multiplying the V_B expression results from referring the incident wave to edge M_1 . This relationship may be seen from Fig. 10 where the phase difference between the two incident waves on edges M_1 and N_1 is the electrical distance $a_1 \cot \theta_{g1} \cos A_{01}$. The resulting doubly diffracted wave from edge M_1 is thus obtained from Eq. (5a) as:

$$\begin{aligned}
(25) \quad & \frac{e^{-j\frac{\pi}{4}}}{2\pi} e^{jk \frac{ra_1}{r+a_1}} \frac{e^{-jk(r+a_1)}}{\sqrt{\frac{r+a_1}{\lambda}}} \left\{ \left(\frac{\frac{1}{n_1} \sin \frac{\pi}{n_1}}{\cos \frac{\pi}{n_1} - \cos \frac{\pi - \theta_{g1} - A_{01}}{n_1}} \right. \right. \\
& \quad \left. \left. - \frac{\frac{1}{n_1} \sin \frac{\pi}{n_1}}{\cos \frac{\pi}{n_1} - \cos \frac{\pi - \theta_{g1} + A_{01}}{n_1}} \right) \right\}
\end{aligned}$$

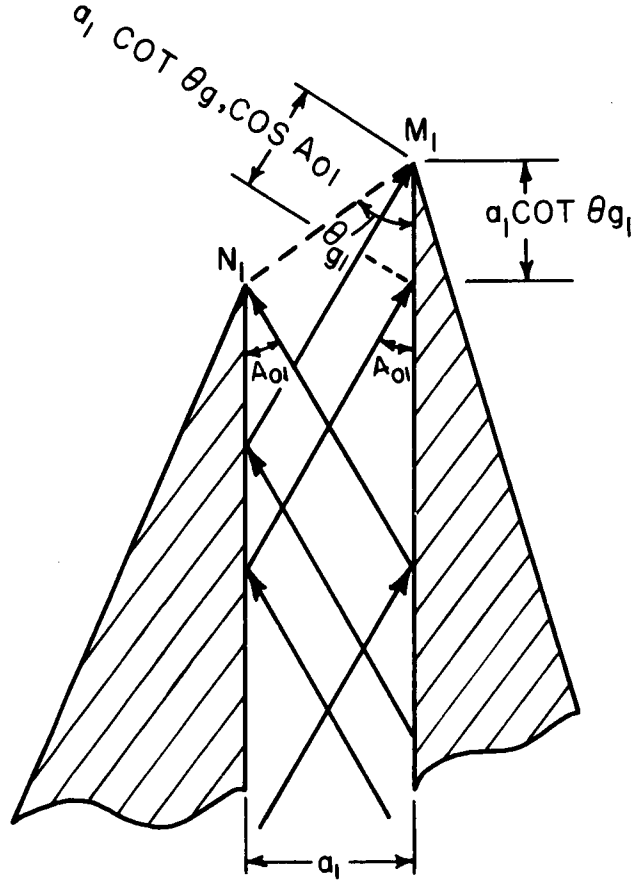


Fig. 10. Phase difference between TE₀₁ incident rays.

$$(25) \quad \times \left[V_B \left(\frac{a_1}{\sin \theta_{g1}}, \frac{3}{2} \pi - E_1 - \theta_{g1}, m_1 \right) - V_B \left(\frac{a_1}{\sin \theta_{g1}}, \frac{3}{2} \pi - E_1 + \theta_{g1}, m_1 \right) \right] \\ \text{cont.} \quad \times e^{jk a_1 \cot \theta_{g1} \cos A_{01}} \quad .$$

Ignoring higher-order diffractions, the electric field intensity radiated in the direction of guide 2 by guide 1 is given in far field form as

$$(26) \quad E_{T1}(\theta_0) = \frac{\sqrt{\lambda} e^{-j\frac{\pi}{4}}}{2\pi} \frac{e^{-jkr}}{\sqrt{r}} \left\{ \frac{\frac{1}{m_1} \sin \frac{\pi}{m_1}}{\cos \frac{\pi}{m_1} - \cos \frac{3/2 \pi - E_1 - A_{01}}{m_1}} \right\}$$

(26)
cont.

$$\begin{aligned}
& - \frac{\frac{1}{m_1} \sin \frac{\pi}{m_1}}{\cos \frac{\pi}{m_1} - \cos \frac{3/2\pi - E_1 + A_{01}}{m_1}} \Bigg) + \left(\frac{\frac{1}{n_1} \sin \frac{\pi}{n_1}}{\cos \frac{\pi}{n_1} - \cos \frac{\pi - \theta_{g1} - A_{01}}{n_1}} \right. \\
& \left. - \frac{\frac{1}{n_1} \sin \frac{\pi}{n_1}}{\cos \frac{\pi}{n_1} - \cos \frac{\pi - \theta_{g1} + A_{01}}{n_1}} \right) e^{jka_1 \cot \theta_{g1} \cos A_{01}} \\
& \times \left[V_B \left(\frac{a_1}{\sin \theta_{g1}}, \frac{3}{2} \pi - E_1 - \theta_{g1}, m_1 \right) \right. \\
& \left. - V_B \left(\frac{a_1}{\sin \theta_{g1}}, \frac{3}{2} \pi - E_1 + \theta_{g1}, m_1 \right) \right] \Bigg\} .
\end{aligned}$$

Guide 1 will then be replaced by a single line source located at edge M_1 that radiates a field given by

$$(27) \quad V_{eq} \frac{e^{-jkr + j\frac{\pi}{4}}}{\sqrt{2\pi r}} = E_{T_1}(\theta_0) = D_{T_1}(\theta_0) \frac{e^{-jkr}}{\sqrt{r}} ,$$

where V_{eq} is the modal voltage of the equivalent line source. The characteristic admittance of the line source is chosen to be that of free space, Y_0 . The modal voltage of the equivalent source is thus given by

$$(28) \quad V_{eq} = \sqrt{2\pi} D_{T_1}(\theta_0) e^{-j\frac{\pi}{4}} .$$

STEP 2: Response of Guide 2 to the equivalent line source.

Reciprocity is again applied to obtain the response of a guide to a line source. The modal voltage received by the line source in Fig. 11(a) with characteristic admittance Y_0 is

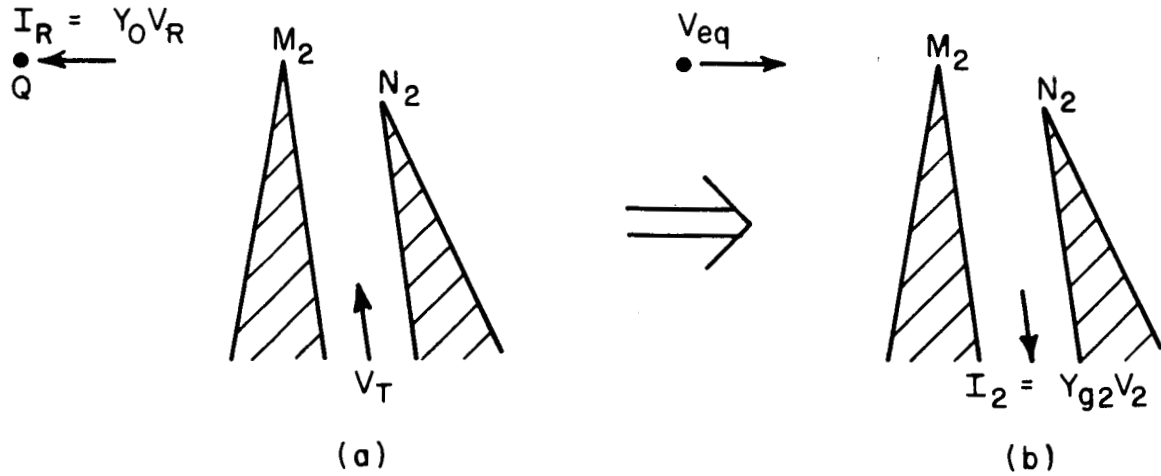


Fig. 11. Response of the TE_{01} receiving guide to the equivalent line source.

$$(29) \quad V_R = \sqrt{\frac{\lambda}{2\pi}} E_T(Q) \quad .$$

The field $E_T(Q)$ at point Q due to guide 2 may be computed by use of Eqs. (1) and (5). The singly diffracted field at point Q from edge M_2 is obtained from Eq. (1) as

$$(30) \quad SD = V_B(D, \frac{3}{2}\pi - E_2 - A_{02}, m_2) - V_B(D, \frac{3}{2}\pi - E_2 + A_{02}, m_2) \quad .$$

The doubly diffracted field from edge M_2 results from the singly diffracted ray from edge N_2 and is given by

$$(31) \quad DD = e^{jka_2 \cot \theta_{g2} \cos A_{02}} \frac{\sqrt{\lambda}}{2\pi} e^{-j\frac{\pi}{4}} \cdot \left(\frac{\frac{1}{n_2} \sin \frac{\pi}{n_2}}{\cos \frac{\pi}{n_2} - \cos \frac{\pi - \theta_{g2} - A_{02}}{n_2}} - \frac{\frac{1}{n_2} \sin \frac{\pi}{n_2}}{\cos \frac{\pi}{n_2} - \cos \frac{\pi - \theta_{g2} + A_{02}}{n_2}} \right)$$

$$(31) \quad \text{cont.} \quad \cdot U_d \left(D, \frac{a_2}{\sin \theta_{g2}}, \frac{3}{2} \pi - E_2, \theta_{g2} \right) .$$

Thus the total field at point Q due to guide 2 is given by

$$(32) \quad E_{T2}(Q) = [V_B(D, \frac{3}{2} \pi - E_2 - A_{02}, m_2) - V_B(D, \frac{3}{2} \pi - E_2 + A_{02}, m_2)] \\ + e^{jka_2 \cot \theta_{g2} \cos A_{02}} e^{-j \frac{\pi}{4}} \frac{e^{jk \left[\frac{a_2 D}{a_2 + D \sin \theta_{g2}} - \left(\frac{a_2}{\sin \theta_{g2}} + D \right) \right]}}{2\pi \sqrt{\frac{a_2 + D \sin \theta_{g2}}{\lambda \sin \theta_{g2}}}} \\ \cdot \left(\frac{\frac{1}{n_2} \sin \frac{\pi}{n_2}}{\cos \frac{\pi}{n_2} - \cos \frac{\pi - \theta_{g2} - A_{02}}{n_2}} - \frac{\frac{1}{n_2} \sin \frac{\pi}{n_2}}{\cos \frac{\pi}{n_2} - \cos \frac{\pi - \theta_{g2} + A_{02}}{n_2}} \right) \\ \cdot \left[V_B \left(\frac{a_2 D}{a_2 + D \sin \theta_{g2}}, \frac{3}{2} \pi - E_2 - \theta_{g2}, m_2 \right) \right. \\ \left. - V_B \left(\frac{a_2 D}{a_2 + D \sin \theta_{g2}}, \frac{3}{2} \pi - E_2 + \theta_{g2}, m_2 \right) \right] ,$$

where the modal voltage of the source, guide 2, is given by

$$(33) \quad V_T = \sqrt{2 a_2 \frac{Y_0}{Y_{g2}} \cos A_{02}} .$$

The modal current I_2 induced in the receiving guide by the equivalent line source, as shown in Fig. 11(b), is given by reciprocity[8] as

$$(34) \quad I_2 = \frac{V_{eq}}{V_T} I_R .$$

The modal voltage V_2 induced in the receiving guide is given by use of Eqs. (28), (29), (33), and (34) as

$$(35) \quad V_2 = \frac{I_2}{Y_{g2}} = \frac{\sqrt{Y_0}}{\sqrt{Y_{g2}}} \frac{\sqrt{\lambda} e^{-j\frac{\pi}{4}}}{\sqrt{2a_2 \cos A_{02}}} D_{T_1}(\theta_0) E_{T_2}(Q) .$$

STEP 3: Mutual coupling

The modal voltage response, V_2 , of guide 2 is given by Eq. (35) for which the source, guide 1, has a modal voltage as given by Eq. (22); i. e.,

$$(36) \quad V_1 = \sqrt{2 a_1 \frac{Y_0}{Y_{g1}} \cos A_{01}} .$$

Thus the TE_{01} mutual coupling between the parallel-plate guides of Fig. 4 is given by

$$(37) \quad \frac{\text{modal voltage received in guide 2}}{\text{modal voltage transmitted in guide 1}} = \frac{V_2}{V_1} = \frac{\sqrt{Y_{g1}}}{\sqrt{Y_{g2}}} \frac{\sqrt{\lambda} e^{-j\frac{\pi}{4}}}{2\sqrt{a_1 a_2 \cos A_{01} \cos A_{02}}} D_{T_1}(\theta_0) E_{T_2}(Q) .$$

$D_{T_1}(\theta_0)$ is the diffraction coefficient of the transmitting guide as given by Eqs. (27) and (28). $E_{T_2}(Q)$ is the field of the receiving guide at point Q as given by Eq. (32). The power coupled between the two guides is given by

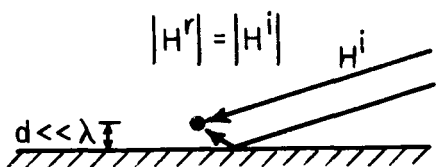
$$(38) \quad \frac{P_2}{P_1} = \left| \frac{V_2}{V_1} \sqrt{\frac{Y_{g2}}{Y_{g1}}} \right|^2 .$$

IV. GROUND PLANE CASE

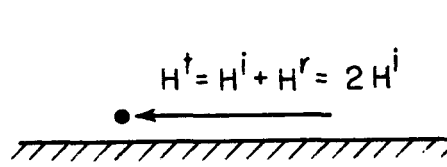
The expressions for coupling which are derived in the previous sections are valid provided the wedge angles for wedges M_1 and M_2 are not too large. Since these expressions neglect the contribution from the intersection of these two wedges they are not accurate if the intersection

is near the line of sight between edges M_1 and M_2 . Typically the intersection should be at least 20° removed from the line of sight. However, the case for which the wedge surfaces coincide to form a ground plane between the guides can be treated for the TEM mode in the same manner as before. TE_{01} coupling for the ground-plane case is quite small; and this analysis predicts zero coupling.

The basic difference between the derivations for coupling with and without ground plane results from the distinction between incident and total fields for grazing incidence on a ground plane. The effective aperture of a magnetic line source on an infinite ground plane is λ/π for non-grazing incidence, as shown in Fig. 12(a). If the effective aperture for grazing incidence is defined as λ/π , then the incident field intensity must be taken as one half of the total field incident on the line source; the other half must be considered as the reflected field as shown in Fig. 12(b).



(a) $P = \frac{\lambda}{\pi} S^i = \frac{\lambda}{\pi} |H^i|^2 Y_0$



(b) $P = \frac{\lambda}{\pi} \left| \frac{1}{2} H^t \right|^2 Y_0$

Fig. 12. Effective aperture of a line source on a ground plane.

In Step 1 of the analysis for TEM coupling in the ground-plane case the transmitting guide is replaced, as shown in Fig. 7, by an equivalent line source located on a ground plane which radiates a field given by

$$(39) \quad \frac{I_{eq} e^{-jkr + j\frac{\pi}{4}}}{\sqrt{\pi r}} = H_{T_1}(\theta_0) = D_{T_1}(\theta_0) \frac{e^{-jkr}}{\sqrt{r}},$$

where the field radiated by the transmitting guide is given by Eq. (11). Thus the modal current of the equivalent line source is given by

$$(40) \quad I_{eq} = \sqrt{\pi} D_{T_1}(\theta_0) e^{-j\frac{\pi}{4}},$$

where a difference of $\sqrt{2}$ with respect to Eq. (13) occurs because the line source on the ground plane has a gain of 2.

In Step 2 of the analysis the response of the receiving guide to a line source located on the ground plane is again determined by use of reciprocity. In the determination of the modal current of the line source due to the guide the field $H_T(Q)$, as given by Eq. (18), represents the total field and hence the effective aperture λ/π of the line source applies to $1/2 H_T(Q)$. Thus the modal current received by the line source in Fig. 8(b) is given by

$$(41) \quad I_R = \frac{1}{2} \sqrt{\frac{\lambda}{\pi}} H_T(Q) ,$$

where $H_T(Q)$ is given by Eq. (18) and applies when the guide transmits with a modal current \sqrt{a} . Hence the response of the line source to the guide and consequently the response of the guide to the line source is given by the modal current ratio

$$(42) \quad \frac{I_R}{I_T} = \frac{1}{2} \sqrt{\frac{\lambda}{\pi a}} H_T(Q) .$$

In Step 3, the previous two steps are combined to determine the coupling between the two guides. Coupling is obtained from Eq. (42) in which the value of I_T is given by the equivalent line source current, I_{eq} , of Eq. (40). Therefore the TEM mode coupling between the two guides in the ground plane case is given by

$$(43) \quad \frac{I_2}{I_1} = \frac{\sqrt{\lambda}}{2\sqrt{a_1 a_2}} D_{T1}(\theta_0) H_{T2}(Q) e^{-j \frac{\pi}{4}}$$

$$= \frac{\lambda}{2\sqrt{a_1 a_2}} \left\{ \frac{\frac{1}{m_1} \sin \frac{\pi}{m_1}}{\cos \frac{\pi}{m_1} - \cos \frac{3/2\pi - E_1}{m_1}} \right.$$

$$\left. + \left(\frac{\frac{1}{n_1} \sin \frac{\pi}{n_1}}{\cos \frac{\pi}{n_1} - \cos \frac{\pi - \theta_{g1}}{n_1}} \right) \times e^{jka_1 \cot \theta_{g1}} \right.$$

(equation continued on next page)

(43)
cont.

$$\begin{aligned}
& \left[V_B \left(\frac{a_1}{\sin \theta_{g1}}, \frac{3}{2} \pi - E_1 - \theta_{g1}, m_1 \right) \right. \\
& \left. + V_B \left(\frac{a_1}{\sin \theta_{g1}}, \frac{3}{2} \pi - E_1 + \theta_{g1}, m_1 \right) \right] \Bigg\} \\
& \times \left\{ V_B \left(D, \frac{3}{2} \pi - E_2, m_2 \right) \right. \\
& + \left(\frac{e^{jk \left[\frac{a_2 D}{a_2 + D \sin \theta_{g2}} - \left(\frac{a_2}{\sin \theta_{g2}} + D \right) \right]}}{2\pi \sqrt{\frac{a_2 + D \sin \theta_{g2}}{\lambda \sin \theta_{g2}}}} \right) \times e^{jka_2 \cot \theta_{g2}} \\
& \times \left(\frac{\frac{1}{n_2} \sin \frac{\pi}{n_2}}{\cos \frac{\pi}{n_2} - \cos \frac{\pi - \theta_{g2}}{n_2}} \right) \times e^{-j \frac{\pi}{4}} \\
& \times \left[V_B \left(\frac{a_2 D}{a_2 + D \sin \theta_{g2}}, \frac{3}{2} \pi - E_2 - \theta_{g2}, m_2 \right) \right. \\
& \left. + V_B \left(\frac{a_2 D}{a_2 + D \sin \theta_{g2}}, \frac{3}{2} \pi - E_2 + \theta_{g2}, m_2 \right) \right] \Bigg\} .
\end{aligned}$$

It is noted that the coupling predicted by the ground-plane case is exactly 6 db lower than that which would be calculated from Eq. (20) for the case of smaller wedge angles.

V. RESULTS

Mutual coupling, as expressed in Eqs. (20) and (37), was computed with a Scatran program for an IBM 7094 digital computer. Measured results were obtained by utilization of wide-angle sectoral horns to simulate infinite parallel plate guides[3]. An E-plane sectoral horn was used to verify TE_{01} coupling and an H-plane sectoral horn was used to verify TEM coupling. The effect of diffraction in the third dimension for these finite apertures was determined by measuring the on-axis coupling between the horns, with their plates contacting so as to eliminate diffraction in the plane of interest. Both calculated and measured results are presented in the following figures. Figures 13 - 22 show influences of various parameters on mutual coupling between guides in the TEM mode, whereas Figs. 23 - 26 apply for guides in the TE_{01} mode. The guide widths of 0.338λ and 0.761λ were chosen to represent the dimensions of a standard X-band waveguide operating at 10 GHz.

Figure 13 shows the effect of wedge angle variations on mutual coupling between guides in the TEM mode. Calculated results are shown for two different guide widths with measured results for only Case (c) (half-plane guides with 0.338λ guide width). The observed trend is that of increase in coupling with increase in wedge angle. For wedge angles approaching 90° , the formulation of Eq. (20) is inaccurate, as previously discussed. However, the formulation for the ground-plane case is given in Eq. (40) and the calculated results are shown in Fig. 14 with one set of experimental verification.

The effects of guide truncation angle on coupling in the TEM mode for half-plane guides are shown in Figs. 15 and 16. For the 0.338λ guide width case (Fig. 15) the trend is as one would expect, i.e. a decrease in coupling for a decrease in guide angle θ_g . For the 0.761λ guide width case (Fig. 16), however, the trend is somewhat different. Calculated far field patterns using the same edge diffraction techniques over the same range of θ_g for the two guides also verifies these trends.

Figure 17 shows the effect of guide width variation on coupling between TEM mode guides with half-plane walls while Fig. 18 is for a TEM mode guide terminated normally by a ground plane. As expected, the coupling decreases with increasing guide width and hence increasing pattern directivity.

Mutual coupling between parallel guides truncated obliquely are shown in Figs. 19 and 20. The configurations are chosen with consideration

for possible array application. Coupling between obliquely truncated guides with skew orientations are given in Figs. 21 and 22 for the half-plane and ground-plane cases. These results illustrate the versatility of the use of edge diffraction techniques to compute coupling.

Coupling as a function of wedge angle for guides in the TE_{01} mode is considered in Fig. 23. Measured results are shown for the half-plane case. Coupling is observed to decrease with increase in wedge angle. For a wedge angle equal to 90° ; i. e. the ground plane case computed coupling is zero for this mode.

The effect of truncation angle variation on coupling between TE_{01} mode guides with half-plane walls is studied in Fig. 24. The formulation of Eq. (37) applies only for $\theta_g > \sin^{-1} \lambda/2a$ as was previously stated. However, the formulation may readily be extended for $\theta_g < \sin^{-1} \lambda/2a$.

Figure 25 shows the effect of guide width variation on coupling between TE_{01} mode guides with half-plane walls while Fig. 26 shows the effect of oblique guide truncation. Trends observed between TEM and TE_{01} guides are seen to be similar.

VI. CONCLUSIONS

The coupling between parallel-plate waveguides is analyzed by edge-diffraction techniques. Theoretical determination of coupling is difficult, if at all possible, by conventional methods. Furthermore, the edge-diffraction method permits the determination of structural effects such as waveguide geometry and orientation on coupling.

Although this analysis is approximate, it is generally accurate except in cases in which a guide truncation angle is nearly equal to the propagation angle of the waveguide mode. Two formulations for coupling are used for the TEM mode; one for moderate-size wedge angles and one for the ground plane case. Coupling was measured for normally truncated guides whose apertures lie in the same plane, for the TEM and TE_{01} half-plane cases, and the TEM ground plane case. These measured values are in good agreement with calculated values.

The analysis given here may be applied to a theoretical study of mutual coupling in an array of parallel-plate waveguides. The total coupling to each guide would be obtained by superposition of the coupling from each of the other elements in the array.

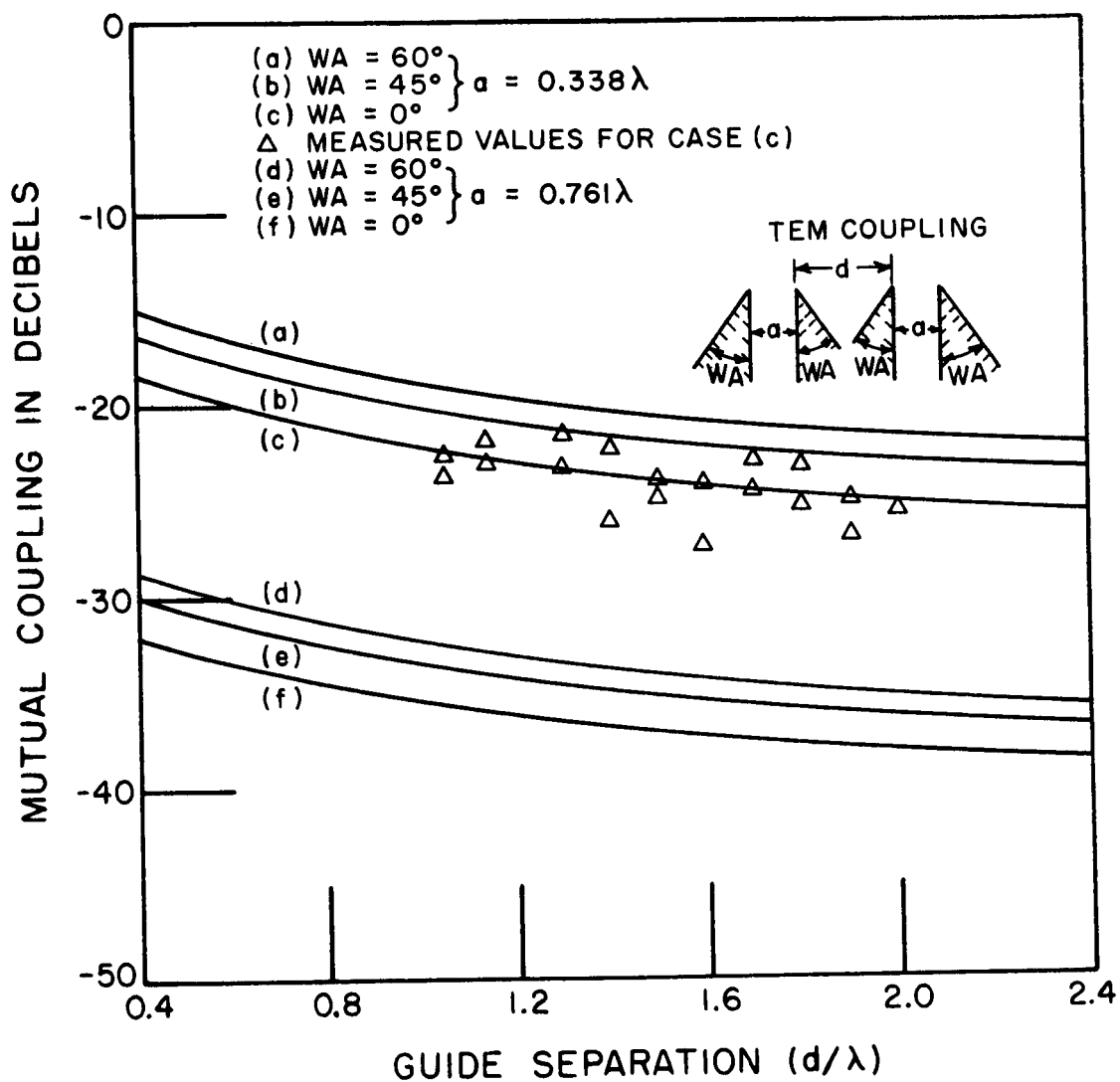


Fig. 13. Effect of wedge angle on TEM mode coupling.

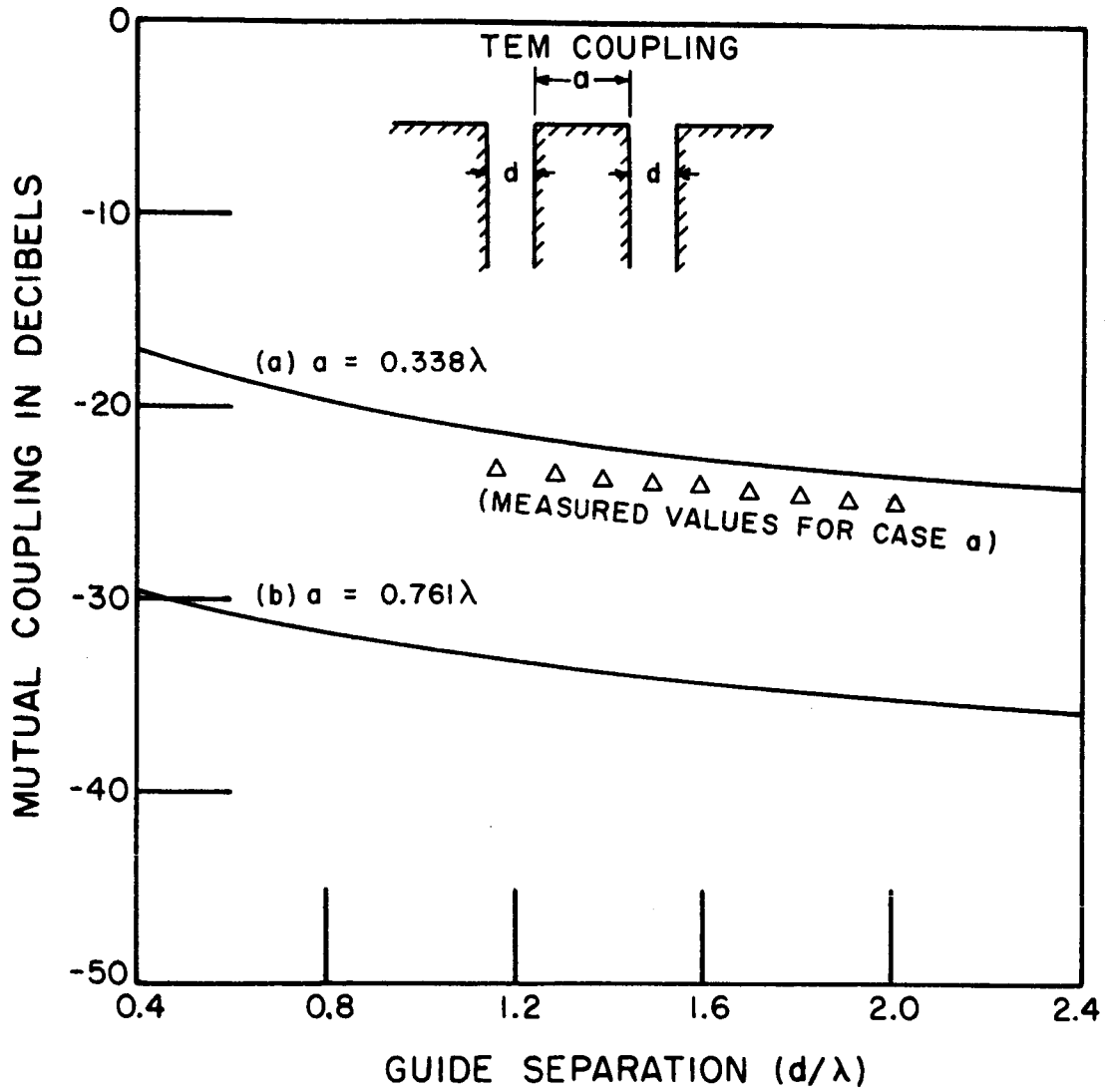


Fig. 14. TEM mode coupling with ground plane.

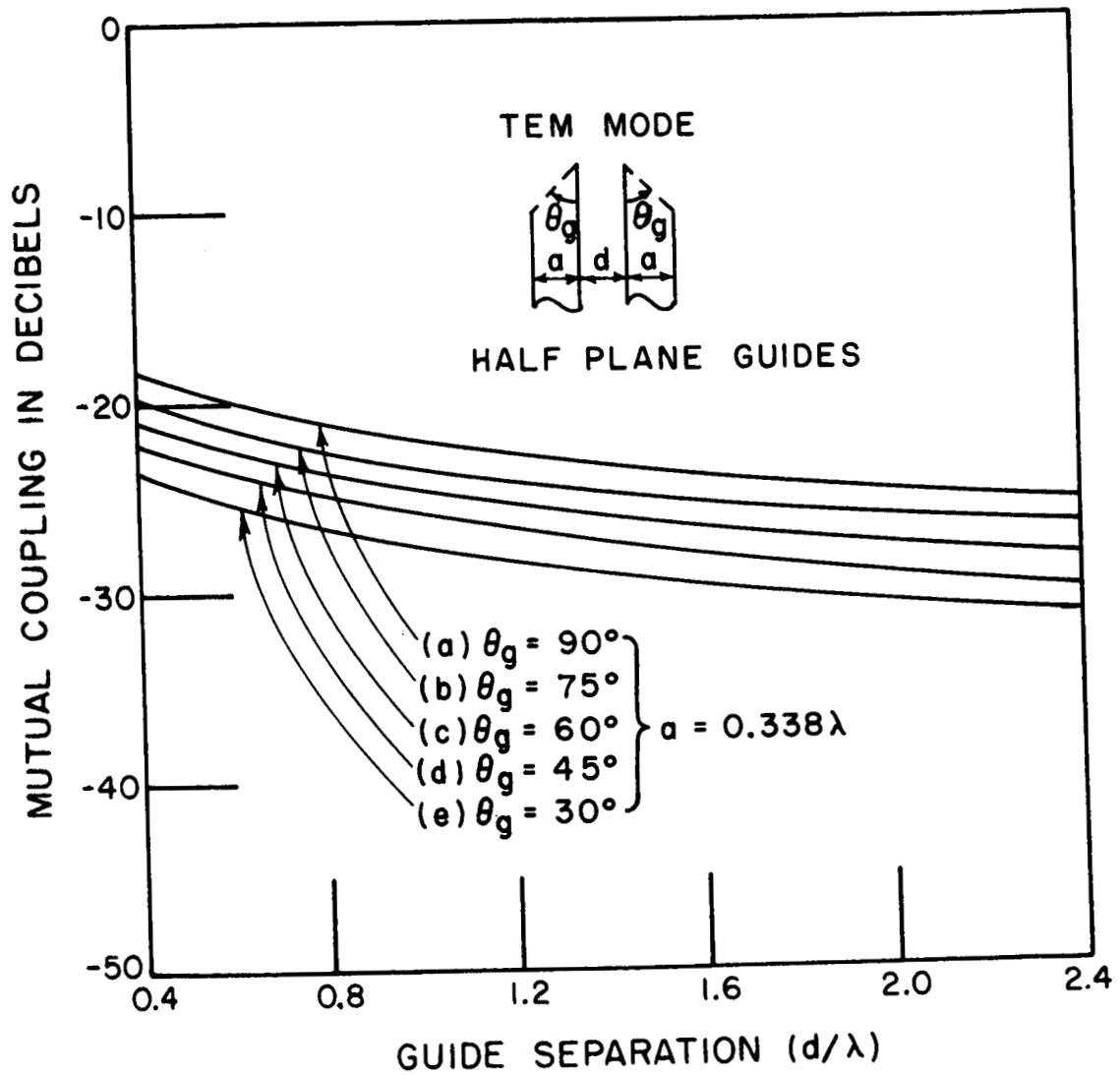


Fig. 15. Effect of guide truncation angle on TEM coupling.

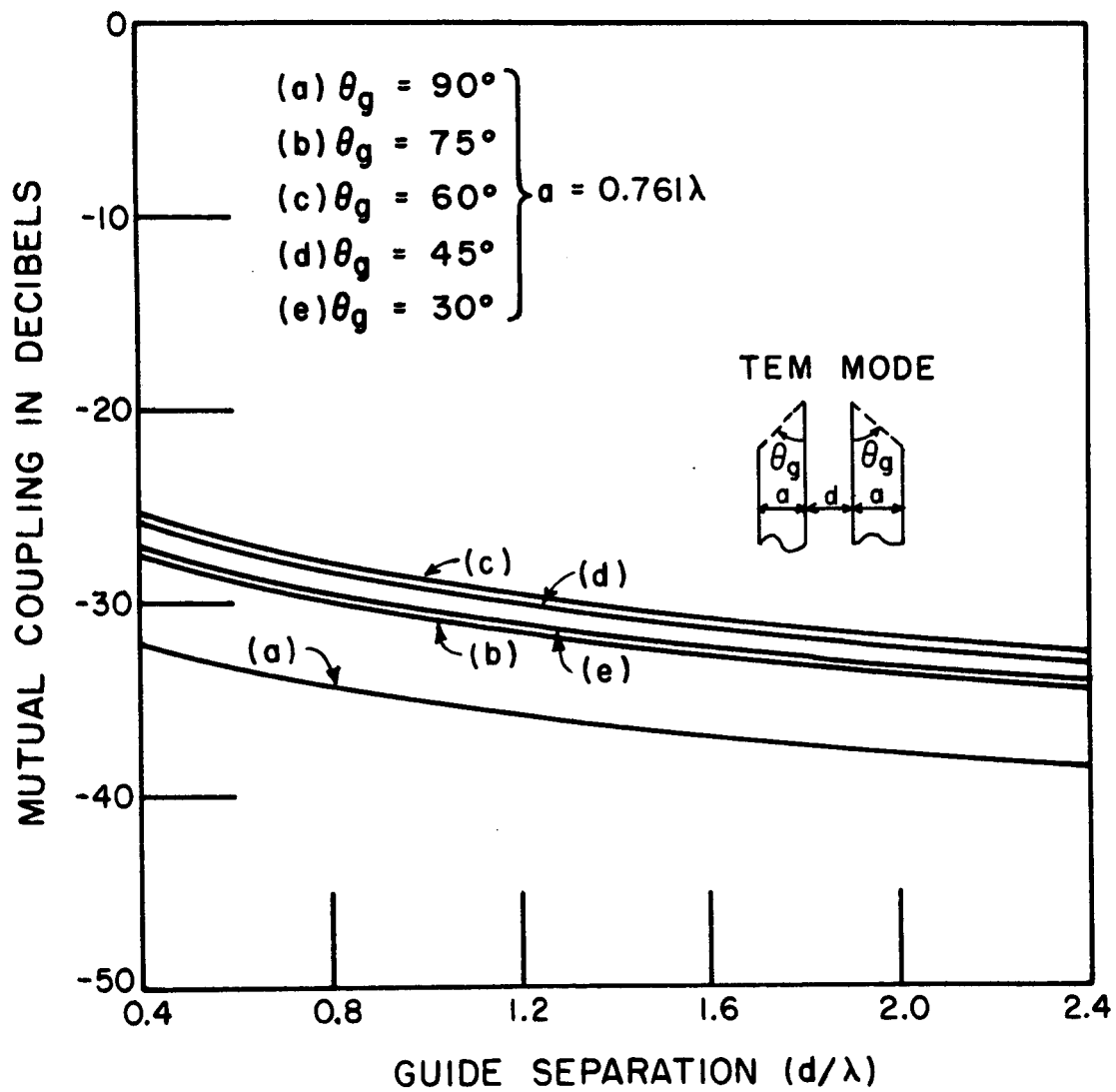


Fig. 16. Effect of guide truncation angle on TEM coupling.

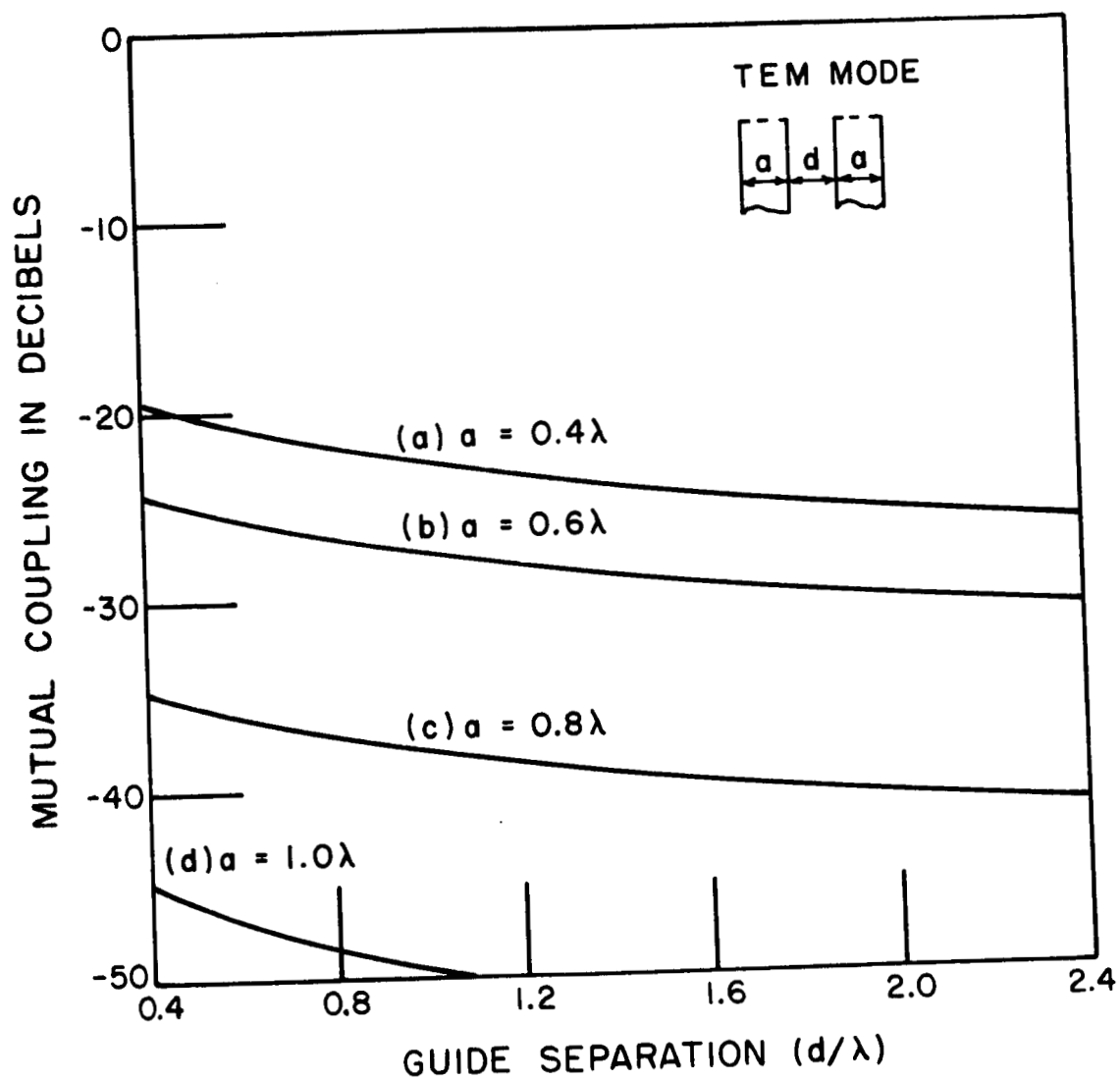


Fig. 17. Effect of guide width on TEM coupling.

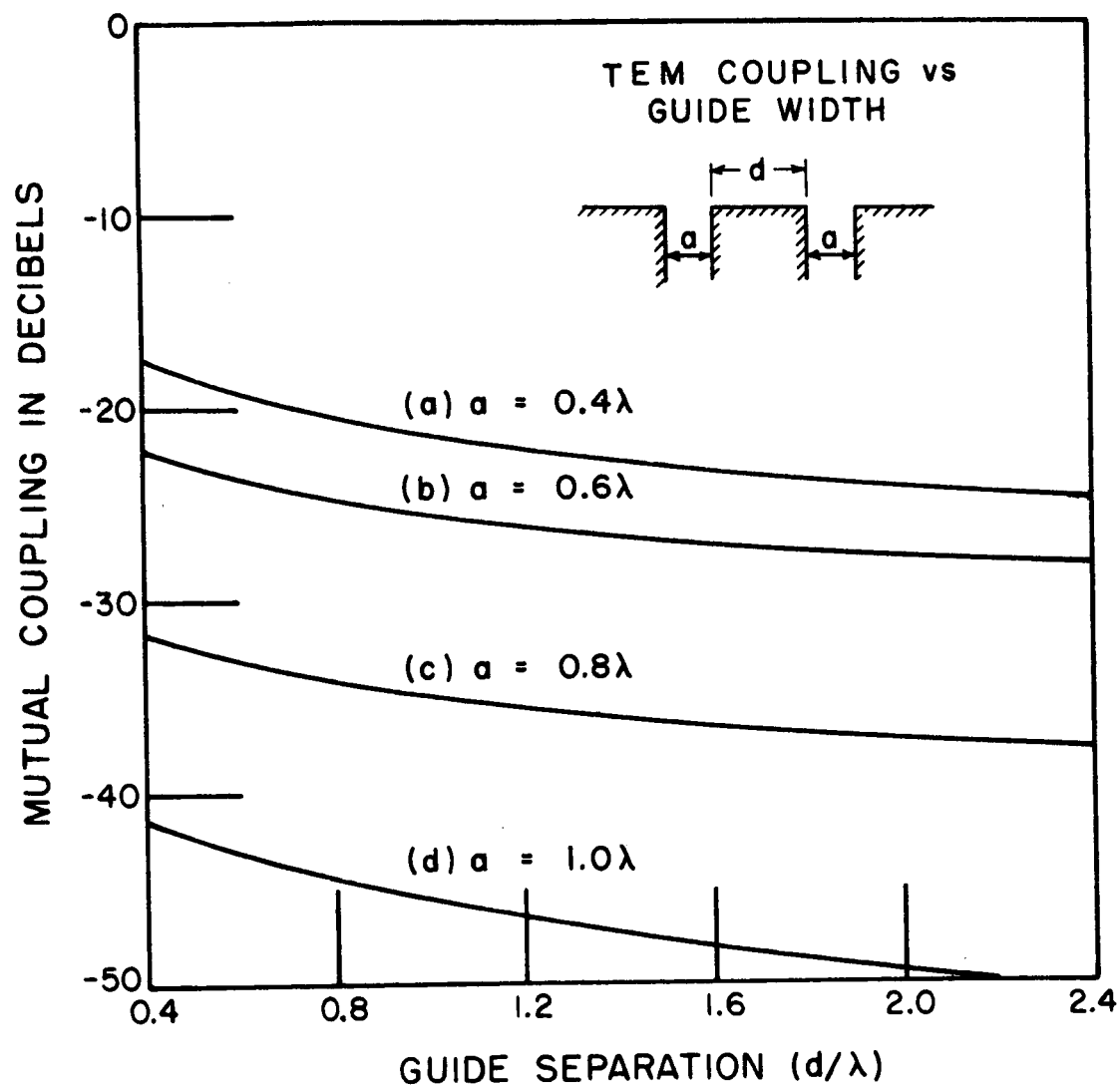


Fig. 18. Effect of guide width variation on TEM coupling.

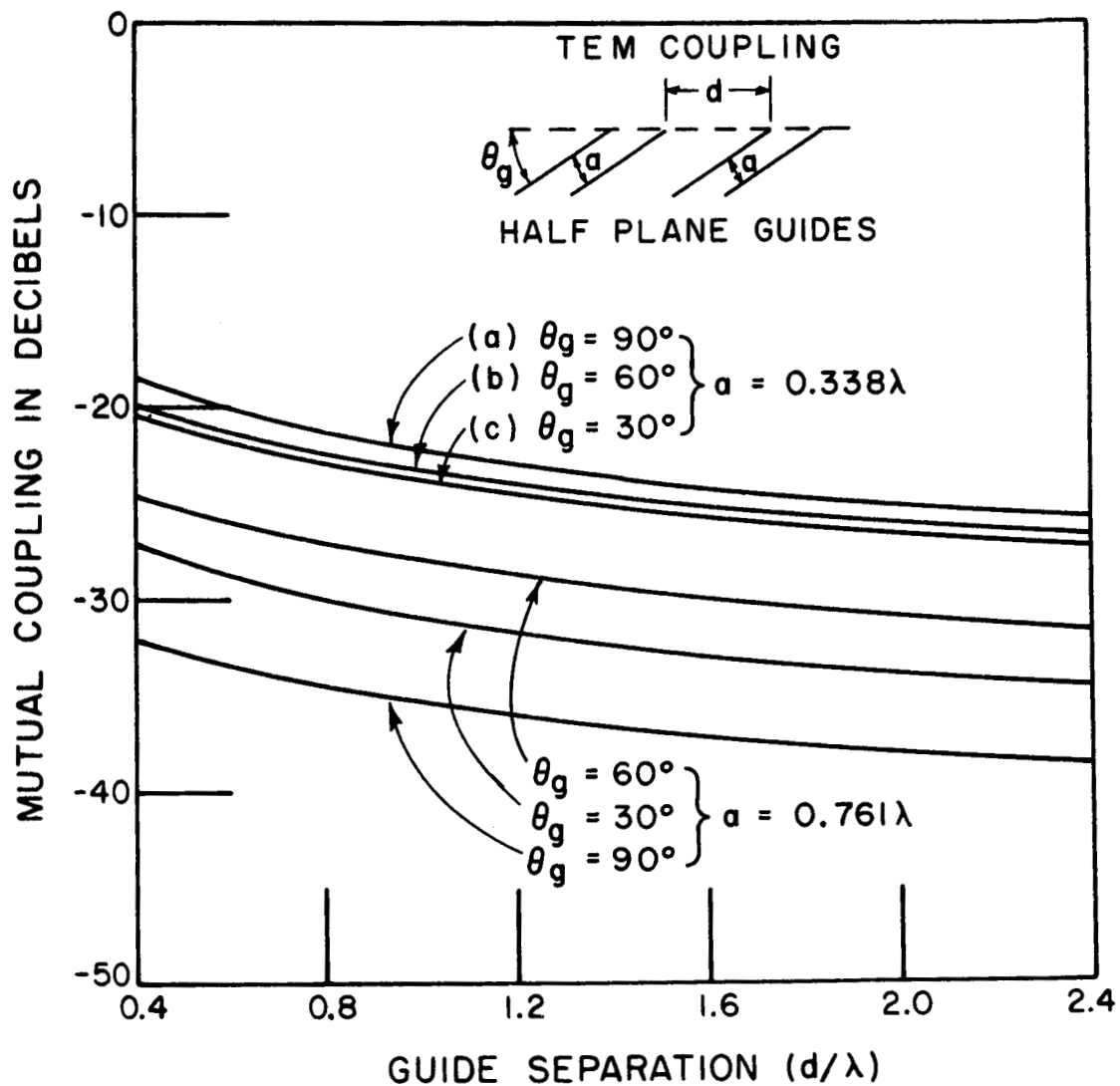


Fig. 19. TEM mode coupling for half-plane parallel guides truncated obliquely.

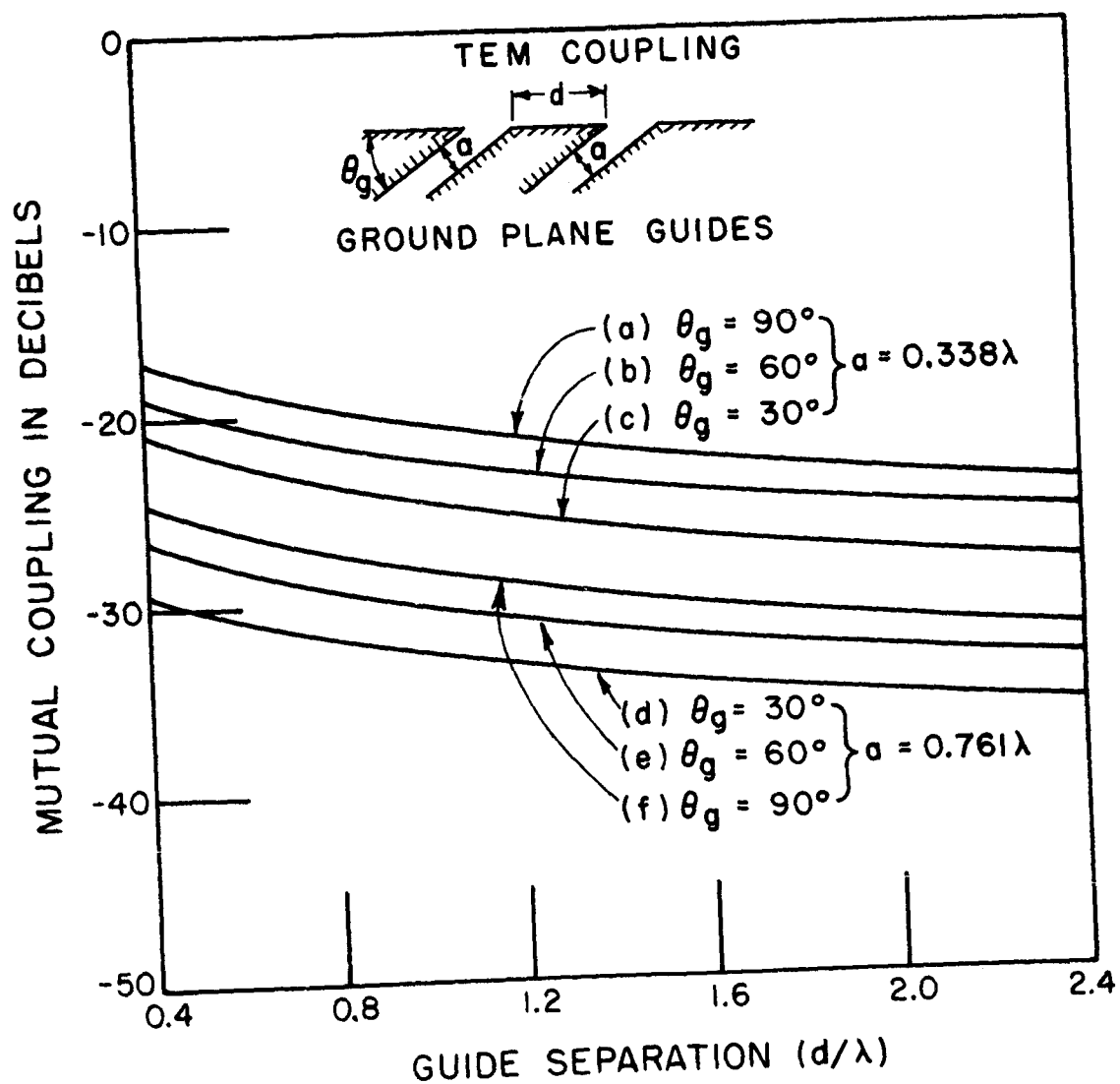


Fig. 20. Coupling between TEM mode parallel guides truncated obliquely by a ground plane.

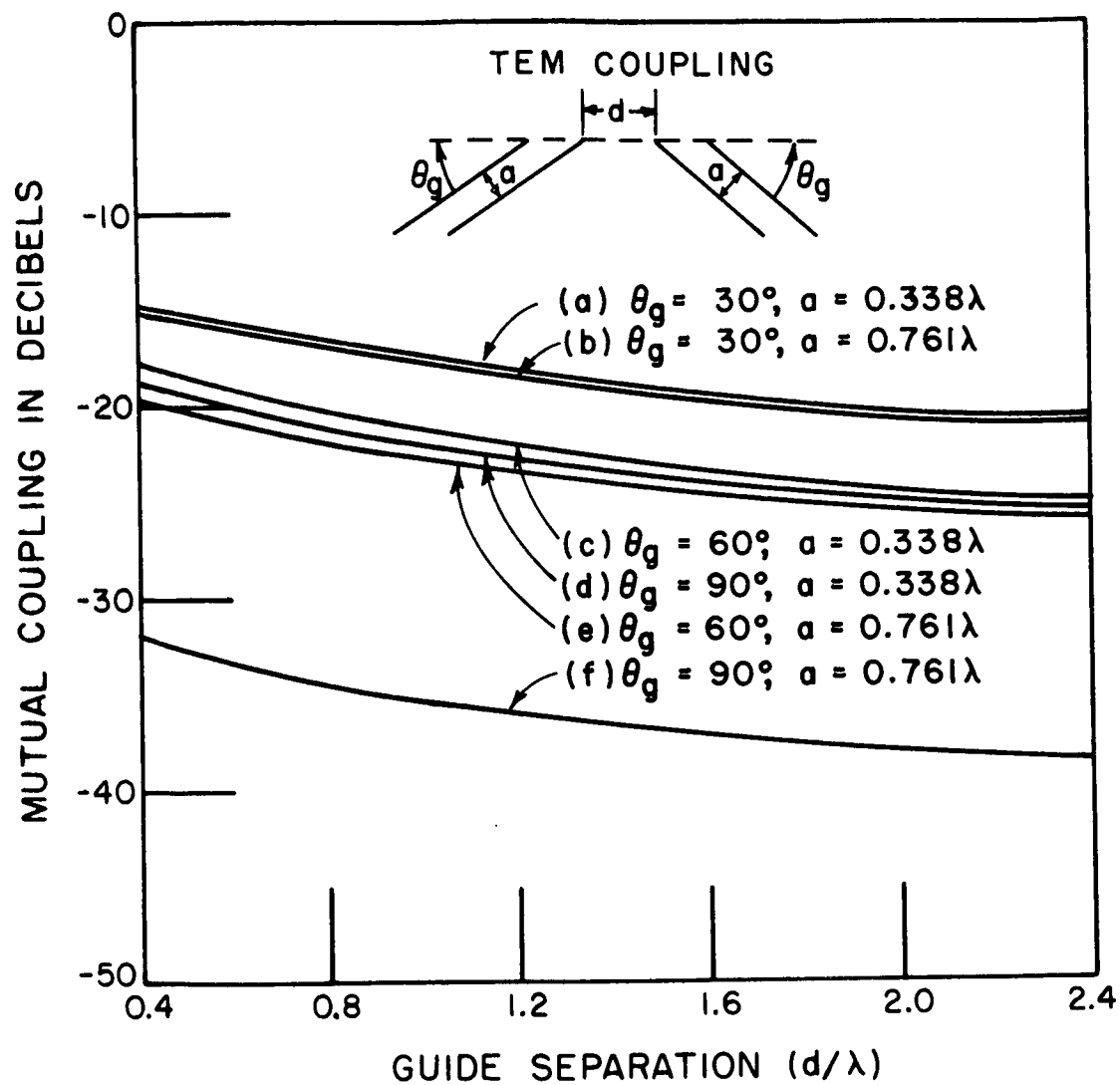


Fig. 21. TEM coupling for half-plane guides.

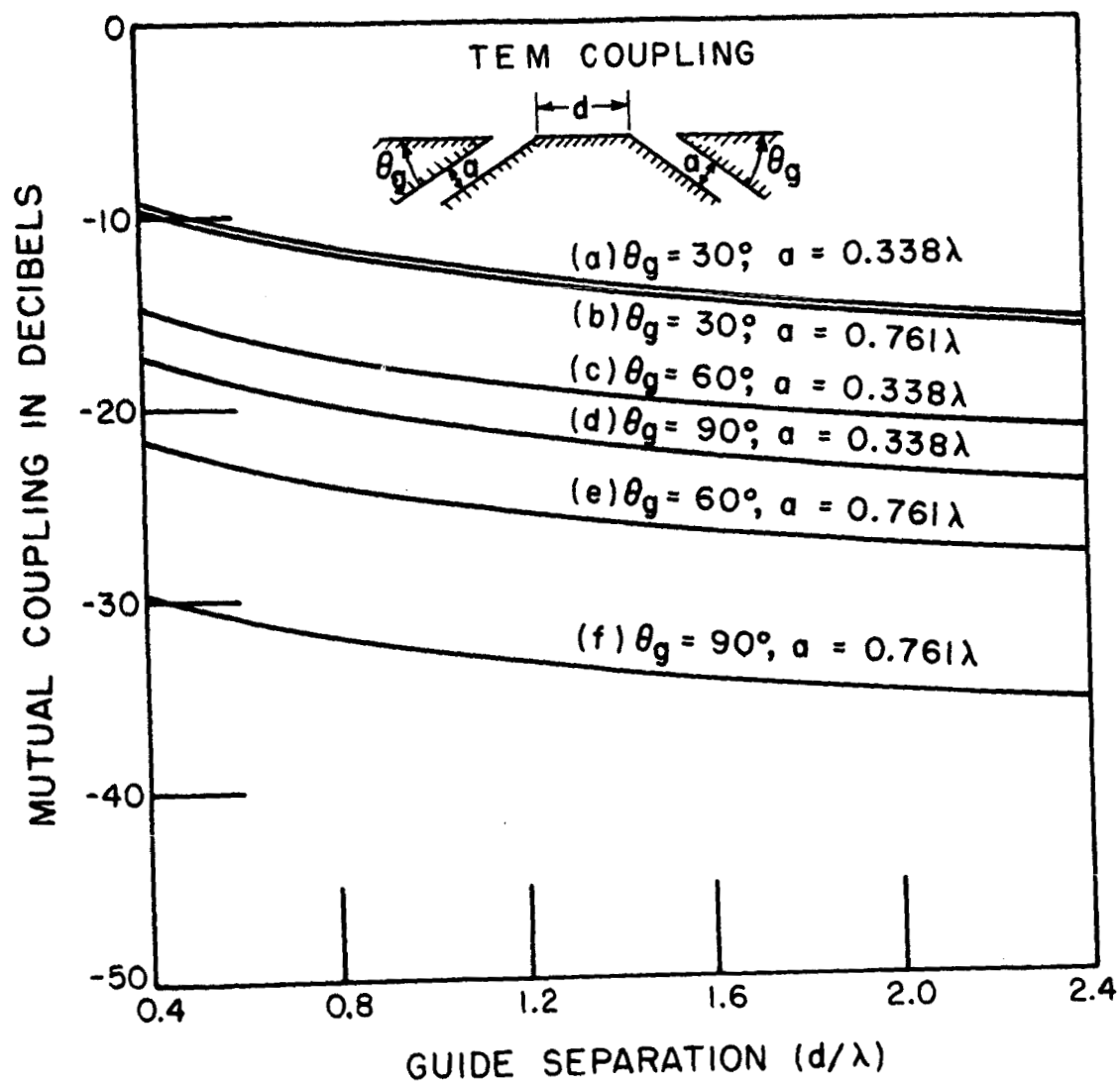


Fig. 22. TEM coupling between ground plane guides.

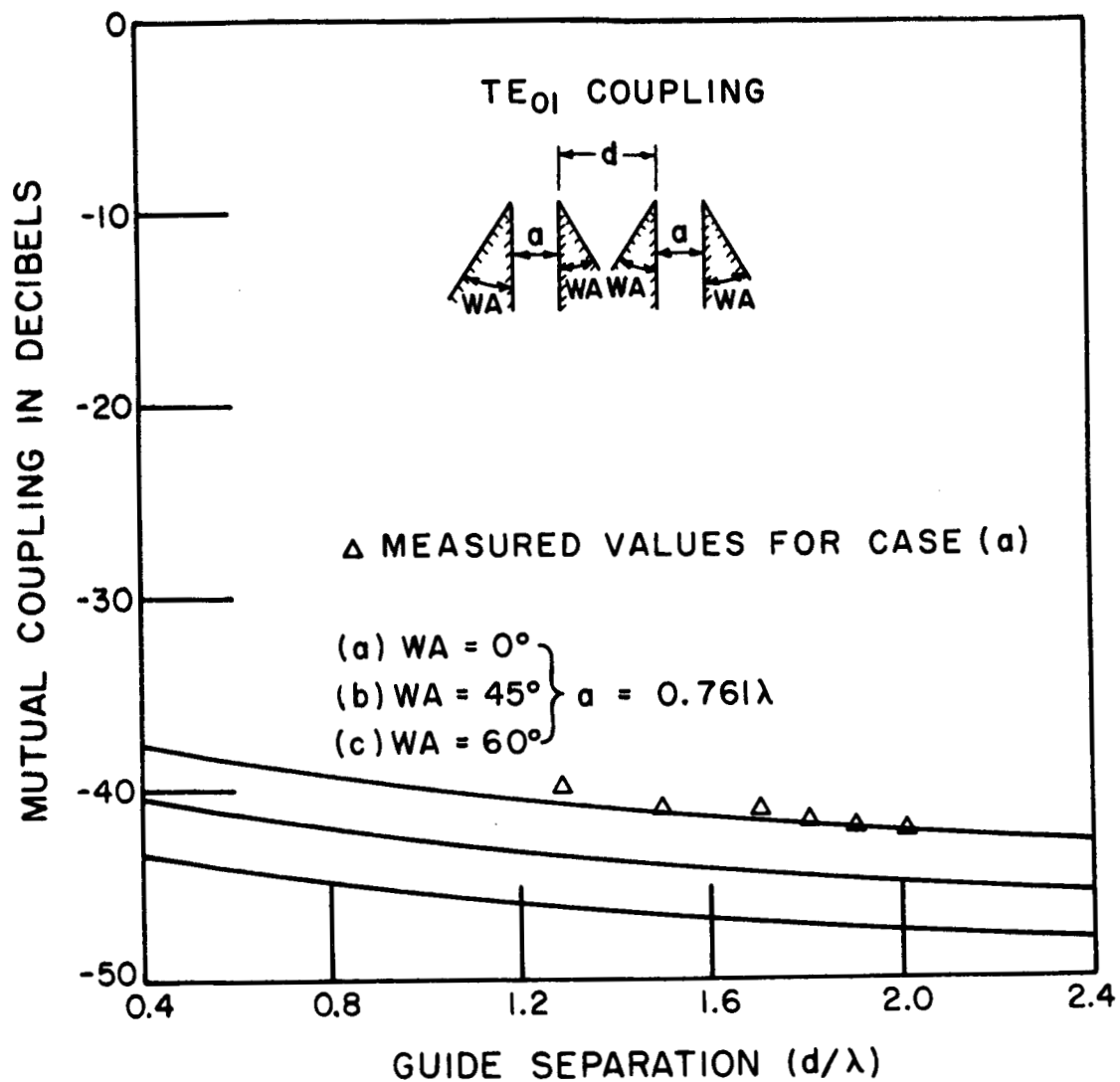


Fig. 23. Effect of wedge angle on TE₀₁ coupling.

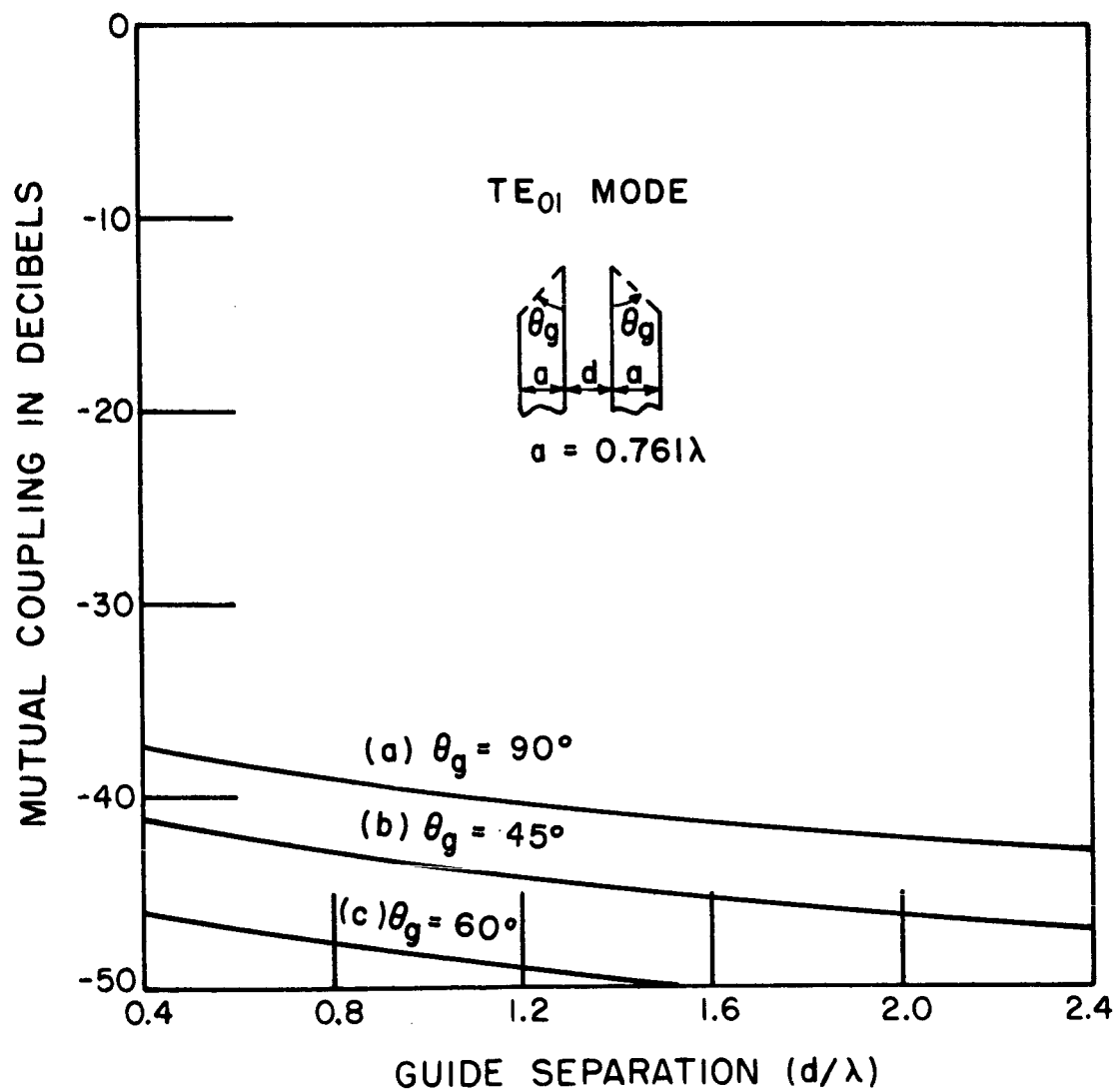


Fig. 24. Effect of truncation angle on TE₀₁ coupling.

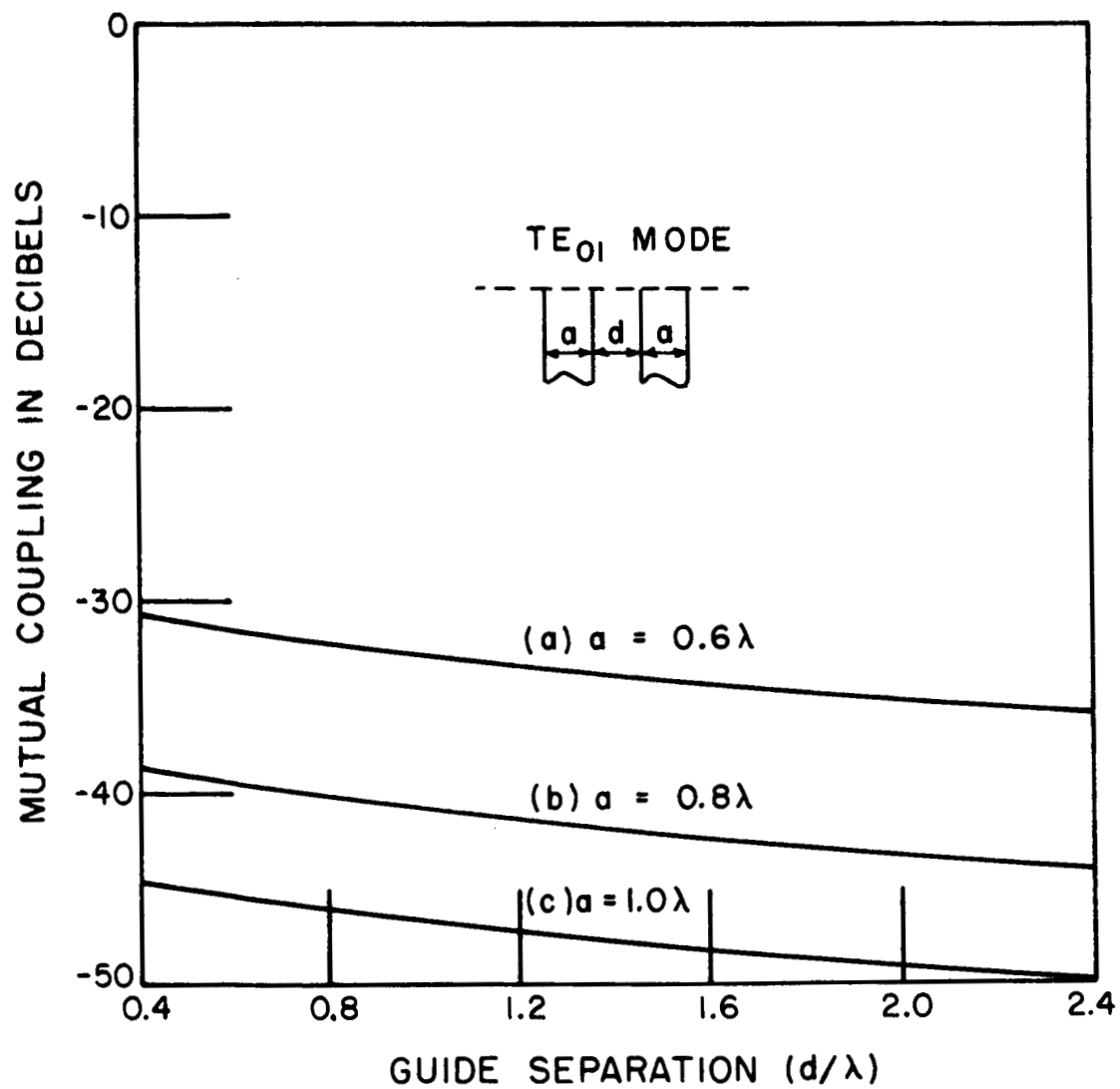


Fig. 25. Effect of guide width on TE_{01} coupling.

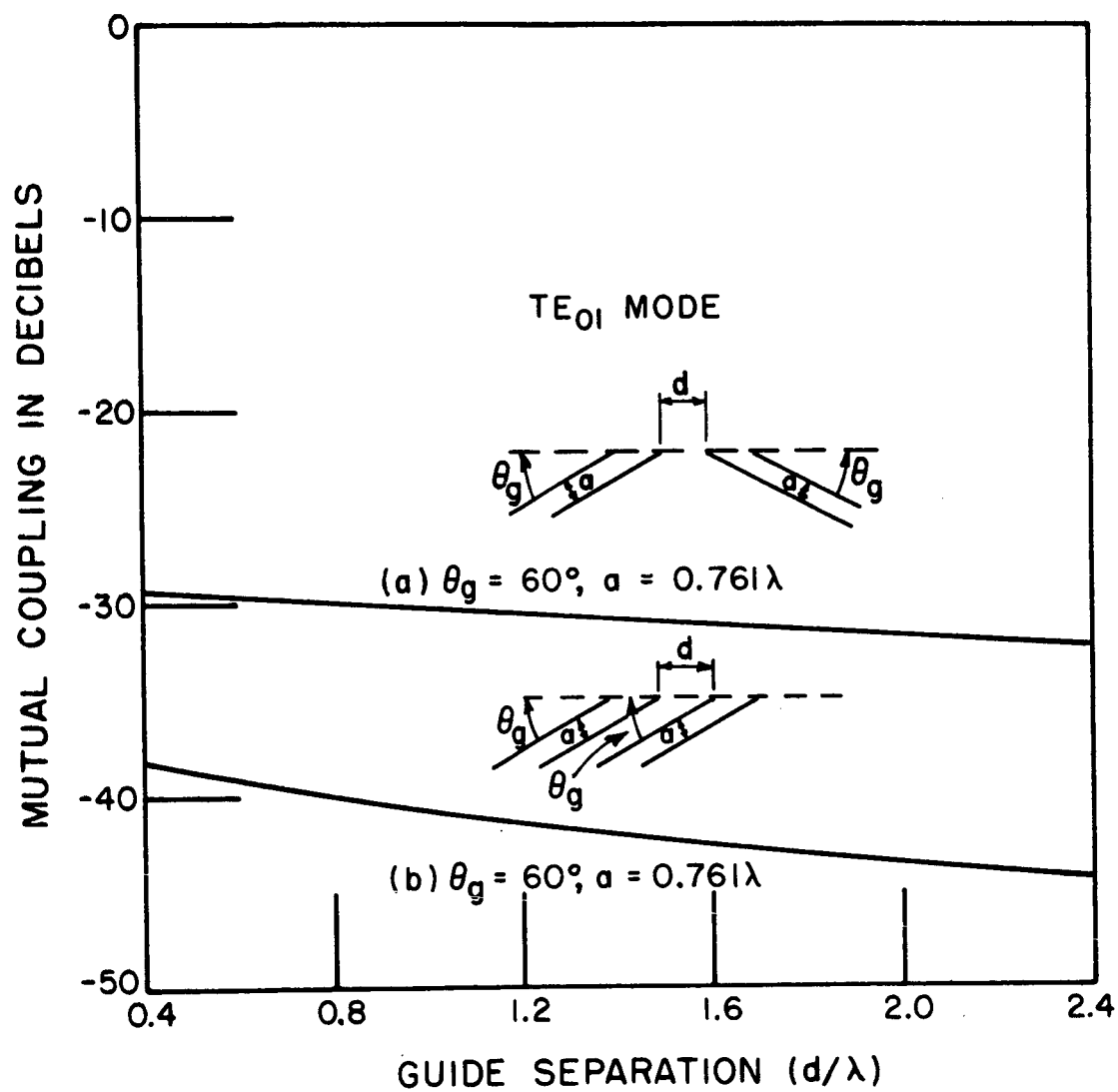


Fig. 26. TE₀₁ mode coupling for half-plane parallel guides truncated obliquely.

APPENDIX A

The diffraction function $V_B(r, \phi)$ for plane-wave incidence has been expressed by Pauli[5] as

$$(44) \quad V_B(r, \phi) = \frac{1}{\sqrt{\pi}} \frac{\sin \frac{\pi}{n} e^{j \frac{\pi}{4}}}{n} \frac{2 \left| \cos \frac{\phi}{2} \right|}{\cos \frac{\pi}{n} - \cos \frac{\phi}{n}} \\ \times e^{jkr \cos \phi} \int_{(akr)^{\frac{1}{2}}}^{\infty} e^{-j\tau^2} d\tau \\ + [\text{higher-order terms}] ,$$

where $a = 1 + \cos \phi$.

The higher-order terms appearing in Eq. (44) are identically equal to zero for the half-plane case, i.e., $n = 2$. For more general values of n , higher-order terms are negligible at large values of kr . The function may be further simplified for large values of akr ; large values of akr imply the point of observation is removed from both the diffracting wedge (r large) and the shadow boundary ($\phi = 180^\circ \rightarrow a = 1 + \cos \phi = 0$). The field, under these conditions, may be expressed by

$$(45) \quad V_B(r, \phi) = \frac{e^{-j \left(kr + \frac{\pi}{4} \right)}}{\sqrt{2\pi kr}} \frac{\frac{1}{n} \sin \frac{\pi}{n}}{\cos \frac{\pi}{n} - \cos \frac{\phi}{n}} + [\text{higher-order terms}] .$$

The diffracted field as expressed by Eq. (45) is that from which the asymptotic diffraction coefficients of the Geometrical Theory of Diffraction[9, 10] are obtained.

For cases in which the higher-order terms of Eq. (44) are significant, an alternative formulation of the problem based on a Bessel function expansion given in Reference 11 may be used. The higher-order terms of the Fresnel integral formulation become significant for values of radial parameter r less than one wavelength. The Bessel

function formulation, which converges rapidly for radial parameters in this region, is given by

$$(46) \quad V(r, \phi) = \frac{1}{n} \sum_{m=0, 1}^{\infty} \epsilon_m j^{\frac{m}{n}} J_{\frac{m}{n}}(kr) \cos \frac{m\phi}{n},$$

where $J_{m/n}(kr)$ is the cylindrical Bessel function of order m/n and ϵ_m is Neumann's number defined by

$$\epsilon_m = \begin{cases} 1 & m = 0 \\ 2 & m \neq 0 \end{cases}.$$

Equation (46) represents the total incident or reflected field where the total field is given by

$$(47) \quad U(r, \psi) = V(r, \psi - \psi_0) + V(r, \psi + \psi_0).$$

The diffracted field may be obtained by simply subtracting the geometric optics field in Eq. (5) from the expression in Eq. (46).

APPENDIX B

The field radiated by a line source in free space with modal current I is given by

$$(48) \quad H = I \frac{e^{-jkr + j\frac{\pi}{4}}}{\sqrt{2\pi r}},$$

where the characteristic impedance Z_0 of the line source is chosen to be that of free space. Thus the magnitude of the field in Eq. (48) corresponds to the power density of a power $P_0 = |I|^2 Z_0$ which is radiated isotropically.

The $e^{-j(kr - \pi/4)}$ phase factor in Eq. (48) results from the fact that the field radiated by the line source modal current must be consistent with the field radiated by a TEM waveguide modal current. A convenient basis for reference is the thin-walled TEM guide with normal truncation ($\theta_g = 90^\circ$). The phase of the field radiated on-axis by this guide with a zero phase modal current is the appropriate phase for the radiated field from a line source with zero phase modal current. The on-axis field of the normally truncated guide is given by the singly diffracted fields from edges M_1 and N_1 because the higher-order diffractions are zero on-axis. The total radiated field on axis is given by [12]

$$(49) \quad \begin{aligned} \lim_{\theta \rightarrow 0} \frac{e^{-j\left(kr + \frac{\pi}{4}\right)}}{2\sqrt{2\pi kr}} & \left[\frac{-1}{\cos \frac{\pi + \theta}{2}} - \frac{e^{jka \cos\left(\theta + \frac{\pi}{2}\right)}}{\cos \frac{\pi - \theta}{2}} \right] \\ &= \lim_{\theta \rightarrow 0} \frac{e^{-j\left(kr + \frac{\pi}{4}\right)}}{2\sqrt{2\pi kr}} e^{-j\frac{ka}{2} \sin \theta} \left[\frac{e^{j\frac{ka}{2} \sin \theta} - e^{-j\frac{ka}{2} \sin \theta}}{\sin \frac{\theta}{2}} \right] \\ &= \frac{e^{-j\left(kr + \frac{\pi}{4}\right)}}{2\sqrt{2\pi kr}} \lim_{\theta \rightarrow 0} \left[e^{-j\frac{ka}{2} \sin \theta} \cdot \frac{2j \sin\left(\frac{ka}{2} \sin \theta\right)}{\sin \frac{\theta}{2}} \right] \\ &= \frac{a}{\sqrt{\lambda r}} e^{-j\left(kr - \frac{\pi}{4}\right)}, \end{aligned}$$

where the associated modal current in the guide is $\sqrt{a} e^{j0}$. Thus the phase factor of the radiated field from a line source in Eq. (48) is the same as that associated with the normally truncated guide in Eq. (49).

REFERENCES

1. Ryan, C. E., Jr., and Rudduck, R. C., "Calculation of Radiation Pattern of a General Parallel Plate TEM Waveguide Aperture," Report 1394-11, 31 December 1963, Antenna Laboratory, The Ohio State University Research Foundation; prepared under Contract AF 33(657)-7829, Aeroanautical Systems Division, Wright-Patterson Air Force Base, Ohio. (AD 433 716).
2. Ryan, C. E., Jr., and Rudduck, R. C., "Calculation of the Radiation Pattern of a General Parallel-Plate Waveguide Aperture for the TEM and TE₀₁ Waveguide Modes," Report 1693-4, 10 September 1964, Antenna Laboratory, The Ohio State University Research Foundation; prepared under Contract N62269-2184, U.S. Naval Air Development Center, Johnsville, Pennsylvania.
3. Dybdal, R. B., "Mutual Coupling between TEM and TE₀₁ Parallel-Plate Waveguide Apertures," Report 1693-5, 15 August 1964, Antenna Laboratory, The Ohio State University Research Foundation; prepared under Contract N62269-2184, U.S. Naval Air Development Center, Johnsville, Pennsylvania.
4. Sommerfeld, A., Optics, Academic Press, Inc., New York, (1954) pp. 245-265.
5. Pauli, W., "On Asymptotic Series for Functions in the Theory of Diffraction of Light," Phys. Rev., 54, 1 December 1938, pp. 924-931.
6. Ohba, Y., "On the Radiation Patterns of a Corner Reflector Finite in Width," IRE Trans. on Antennas and Propagation, AP-11, No. 2, (March, 1963), pp. 127-132.
7. Born, M., and Wolf, E., Principles of Optics, The MacMillan Company, New York (1964), Second (Revised) Edition, pp. 580-584.
8. Harrington, R. F., Time-Harmonic Electromagnetic Fields, McGraw-Hill Book Company, Inc., York (1961) pp. 116-120.
9. Keller, J. B., "Diffraction by an Aperture," J. Appl. Phys., 28, No. 4, (April, 1957) pp. 426-444.

10. Keller, J.B., "Geometrical Theory of Diffraction," J. Opt. Soc. Am., 52, No. 2, (February, 1962) pp. 116-130.
11. Harington, R.F., op. cit., pp. 238-242.
12. Rudduck, R.C., "Application of Wedge Diffraction to Antenna Theory," Report 1691-13, 30 June 1965, Antenna Laboratory, The Ohio State University Research Foundation; prepared under Grant NsG-448, National Aeronautics and Space Administration, Office of Grants and Research Contracts, Washington, D.C.